Developmental Cell
Article

Control of Epithelial Cell Migration and Invasion by the IKKβ- and CK1α-Mediated Degradation of RAPGEF2

Roberto Magliozzi,[1] Teck Yew Low,[2,3] Bart G.M.W. Weijts,[4] Tianhong Cheng,[1] Emma Spanjaard,[1] Shabaz Mohammed,[2,3] Anouk van Veen,[6] Huib Ovaa,[5] Johan de Rooij,[1] Fried J.T. Zwartkruis,[6] Johannes L. Bos,[6] Alain de Bruin,[4] Albert J.R. Heck,[2,3] and Daniele Guardavaccaro[1,*]

[1]Hubrecht Institute-KNAW and University Medical Center Utrecht, Uppsalalaan 8, 3584 CT Utrecht, The Netherlands
[2]Biomolecular Mass Spectrometry and Proteomics, Bijvoet Center for Biomolecular Research and Utrecht Institute for Pharmaceutical Sciences, Utrecht University, Padualaan 8, 3584 CH Utrecht, The Netherlands
[3]The Netherlands Proteomics Center, Padualaan 8, 3584 CH Utrecht, The Netherlands
[4]Department of Pathobiology, Faculty of Veterinary Medicine, Utrecht University, Yalelaan 1, 3584 CL Utrecht, The Netherlands
[5]Division of Cell Biology, The Netherlands Cancer Institute, Plesmanlaan 121, 1066 CX Amsterdam, The Netherlands
[6]Department of Physiological Chemistry and Center for Biomedical Genetics, University Medical Center Utrecht, Universiteitsweg 100, 3584 CG Utrecht, The Netherlands
*Correspondence: d.guardavaccaro@hubrecht.eu
http://dx.doi.org/10.1016/j.devcel.2013.10.023

SUMMARY

Epithelial cell migration is crucial for the development and regeneration of epithelial tissues. Aberrant regulation of epithelial cell migration has a major role in pathological processes such as the development of cancer metastasis and tissue fibrosis. Here, we report that in response to factors that promote cell motility, the Rap guanine exchange factor RAPGEF2 is rapidly phosphorylated by I-kappa-B-kinase-β and casein kinase-1α and consequently degraded by the proteasome via the $SCF^{\beta TrCP}$ ubiquitin ligase. Failure to degrade RAPGEF2 in epithelial cells results in sustained activity of Rap1 and inhibition of cell migration induced by HGF, a potent metastatic factor. Furthermore, expression of a degradation-resistant RAPGEF2 mutant greatly suppresses dissemination and metastasis of human breast cancer cells. These findings reveal a molecular mechanism regulating migration and invasion of epithelial cells and establish a key direct link between IKKβ and cell motility controlled by Rap-integrin signaling.

INTRODUCTION

Epithelial cell migration and invasiveness are crucial for morphogenesis during embryonic development and for tissue regeneration. In these processes, epithelial cells lose cell-cell adhesion, develop a mesenchymal cell polarity and, eventually, acquire a highly motile phenotype that enables the invasion of surrounding tissues (Thiery, 2002; Yang and Weinberg, 2008). This biological process, known as epithelial-mesenchymal transition (EMT), has been implicated in diseases such as fibrosis and carcinoma development. Understanding the molecular mechanisms controlling epithelial cell migration is key to develop strategies that may have clinical potential.

Rap, a small guanosine triphosphatase (GTPase) of the Ras family, is a major regulator of cell polarity, adhesion, and migration (Boettner and Van Aelst, 2009; Bos, 2005). It was originally identified as a protein able to revert the transformed phenotype of K-Ras (Kitayama et al., 1989). Biochemical and genetic studies in various model systems have revealed that Rap is a potent activator of integrins (Duchniewicz et al., 2006; Katagiri et al., 2000; Reedquist et al., 2000; Sebzda et al., 2002). Indeed, a number of growth factors and cytokines stimulate integrin-mediated cell adhesion through the activation of Rap. In addition, Rap is required for the formation and maintenance of E-cadherin-mediated cell-cell adhesion independently of its effects on integrins (Hogan et al., 2004; Knox and Brown, 2002; Kooistra et al., 2007; Price et al., 2004).

As other small GTPases, Rap acts as a molecular switch by cycling between inactive GDP-bound and active GTP-bound forms. The transition between these two conformations is tightly controlled by specific guanine nucleotide exchange factors (GEFs), which promote the conversion from the inactive GDP-bound conformation into the active GTP-bound conformation and GTPase-activating proteins (GAPs), which stimulate the intrinsic hydrolytic GTPase activity accelerating the conversion into the inactive GDP-bound form. Rap activity is regulated by a multitude of extracellular signals, which control distinct Rap GEFs and GAPs (Pannekoek et al., 2009). Among them, RAPGEF2 (also known as PDZGEF1, CNRASGEF, NRAPGEP, RA-GEF-1) specifically activates Rap1 and its close relative Rap2 in vitro and in vivo by stimulating GDP-GTP exchange (de Rooij et al., 1999; Kuiperij et al., 2003; Liao et al., 1999; Ohtsuka et al., 1999; Rebhun et al., 2000). Genetic approaches have shown that the *Caenorhabditis elegans* homolog of RAPGEF2, *pxf-1*, is required for Rap-mediated maintenance of epithelial integrity (Pellis-van Berkel et al., 2005). In *Drosophila*, loss of function mutants of *dPDZGEF/Dizzy* display defective development of various organs including eye, wing, and ovary (Lee et al., 2002). In particular, dPDZGEF controls the formation of

adherens junctions during furrow formation in the ventral epithelium (Spahn et al., 2012). Moreover, deletion of *dPDZGEF* results in loss of both germline and somatic stem cells due to an impairment of adherens junctions at the hub-stem cell interface (Wang et al., 2006). *RAPGEF2*$^{-/-}$ mouse embryos die between E11.5 and E12.5 with severe organogenesis defects, indicating that RAPGEF2 is essential for embryonic development in mice (Bilasy et al., 2009; Satyanarayana et al., 2010; Wei et al., 2007). Altogether, these genetic studies indicate that RAPGEF2 plays a fundamental role in the development and maintenance of epithelia, however, the molecular mechanisms that regulate RAPGEF2 levels and functions remain largely unknown.

SCF ubiquitin ligases target key cellular regulatory proteins for ubiquitin-mediated proteolysis (Cardozo and Pagano, 2004; Jin et al., 2004). They are composed of the core subunits Skp1, Cul1, Rbx1, and one of many F-box proteins that serve as specific substrate-receptor subunits. SCF$^{\beta TrCP}$ has been implicated in the degradation of proteins controlling cell cycle progression, apoptosis, circadian rhythms, and differentiation (Frescas and Pagano, 2008). All substrates of SCF$^{\beta TrCP}$ contain a conserved destruction motif with the consensus DSGXX(X)S, which, once phosphorylated, mediates the binding to the WD40 β-propeller structure of βTrCP. Mammals express two paralogous βTrCP proteins (βTrCP1, also known as FBXW1, and βTrCP2, also called FBXW11), yet their biochemical properties are indistinguishable. We will therefore use the term βTrCP to refer to both, unless specified otherwise.

Here, we show that, in response to metastatic factors, RAPGEF2 is rapidly phosphorylated by CK1α on a conserved degron and ubiquitylated by SCF$^{\beta TrCP}$. CK1α-mediated phosphorylation of RAPGEF2 is stimulated by IKKβ, which phosphorylates RAPGEF2 on Ser1254. RAPGEF2 ubiquitylation triggers its proteasome-dependent degradation, enabling inactivation of Rap1 and induction of cell motility. Remarkably, inhibition of RAPGEF2 proteolysis blocks migration of epithelial cells and suppresses metastasis of breast cancer cells. Thus, CK1α- and IKKβ-dependent degradation of RAPGEF2 represents a critical event required for epithelial cell migration and invasion.

RESULTS

Rapid βTrCP-Dependent Degradation of RAPGEF2 in Response to Stimuli that Induce Cell Migration

To identify substrates of the SCF$^{\beta TrCP}$ ubiquitin ligase, we used an immunoaffinity assay followed by mass spectrometry analysis (Kruiswijk et al., 2012; Low et al., 2013). HEK293T cells were transfected with FLAG-HA epitope-tagged βTrCP2 and treated with the proteasome inhibitor MG132. Proteins that coimmunoprecipitated with FLAG-HA-βTrCP2 were analyzed by liquid chromatography-tandem mass spectrometry. We recovered 14 peptides corresponding to the Rap guanine nucleotide exchange factor RAPGEF2 (Figure S1A available online). We then followed the reciprocal approach and immunopurified FLAG-HA epitope-tagged RAPGEF2 from HEK293T cells. We identified 7, 14, 3, 2, and 1 peptides derived from the SCF subunits βTrCP1, βTrCP2, Skp1, Cul1, and Rbx1, respectively (Figure S1B). In addition, peptides corresponding to the small GTPases Rap1 (isoforms A and B) and Rap2 (isoforms B and C) were detected in the RAPGEF2 immunopurification (Figure S1C). Of note, we never observed other members of the Ras family of small G-proteins when we used RAPGEF2 as bait.

To verify the specificity of the βTrCP-RAPGEF2 binding, we immunoprecipitated a number of FLAG epitope-tagged F-box proteins as well as the related proteins Cdh1 and Cdc20 from HEK293T cells and examined their ability to pull-down endogenous RAPGEF2. βTrCP1 and its paralog βTrCP2 coimmunoprecipitated with endogenous RAPGEF2 (Figure 1A), whereas other members of the FBXW family of F-box proteins, FBXW2, FBXW4, FBXW5, FBXW7, FBXW8, or the APC/C activators Cdh1 and Cdc20 (also containing WD40 repeats) did not. A complex with the endogenous βTrCP and RAPGEF2 proteins was also observed (Figure 1B).

It has been shown that the WD40 β-propeller structure of βTrCP is required for the interaction with its substrate proteins and that mutation of a specific arginine residue (Arg447 of human βTrCP2, isoform C) in the WD40 repeats abolishes both the binding and ubiquitin conjugation of the substrate (Kruiswijk et al., 2012; Wu et al., 2003). To determine if the WD40 β-propeller structure of βTrCP is responsible for the binding to RAPGEF2, we expressed in HEK293T cells wild-type βTrCP2 and the βTrCP2(R447A) mutant, which were then immunoprecipitated. Whereas wild-type βTrCP2 immunoprecipitated endogenous RAPGEF2 and the established substrate β-catenin, the βTrCP2(R447A) mutant did not (Figure 1C).

To test whether RAPGEF2 is a substrate of the SCF$^{\beta TrCP}$ ubiquitin ligase, we reconstituted the ubiquitylation of RAPGEF2 in vitro. βTrCP1, but not an inactive βTrCP1(ΔF box) mutant, was able to efficiently ubiquitylate RAPGEF2 (Figure 1D).

Before examining a putative function of the SCF$^{\beta TrCP}$ ubiquitin ligase in targeting RAPGEF2 for degradation, we sought to find under which condition RAPGEF2 is degraded in the cell. As Rap1 is a key mediator of cell adhesion, we hypothesized that RAPGEF2 may be downregulated in response to stimuli that disrupt cell adhesion and induce cell migration. To test this hypothesis, we analyzed RAPGEF2 protein levels in epithelial Madin-Darby canine kidney (MDCK) cells treated with hepatocyte growth factor/scatter factor (HGF/SF). This is a well-established in vitro model system that has been extensively used to study the mechanisms by which epithelial cells become migratory, mesenchymal-like cells. HGF is known to induce centrifugal spreading of MDCK cell colonies, loss of cell-cell adhesion, and increase in cell motility without stimulating cell growth (Gherardi et al., 1989; Stoker et al., 1987; Stoker and Perryman, 1985; Tanimura et al., 1998). Figure 1E shows that RAPGEF2 levels rapidly decreased in response to HGF. The proteasome inhibitor MG132 prevented the decrease of RAPGEF2, indicating that RAPGEF2 degradation is mediated by the proteasome. RAPGEF2 destruction was also triggered following treatment with phorbol-12-myristate-13-acetate (PMA) (Figure 1F), which is known to induce a marked scattering of MDCK cells without affecting significantly cell proliferation (Rosen et al., 1991; Tanimura et al., 1998), but not in response to a number of other growth factors, such as epidermal growth factor (EGF) or insulin-like growth factor (IGF), which do not induce scattering of MDCK cells (Tanimura et al., 1998) (Figures S1D and S1E). Proteasome-dependent degradation of RAPGEF2 was observed upon HGF treatment of human epithelial kidney HEK293 cells (Figure S1F), which form epithelial layers similar to MDCK cells

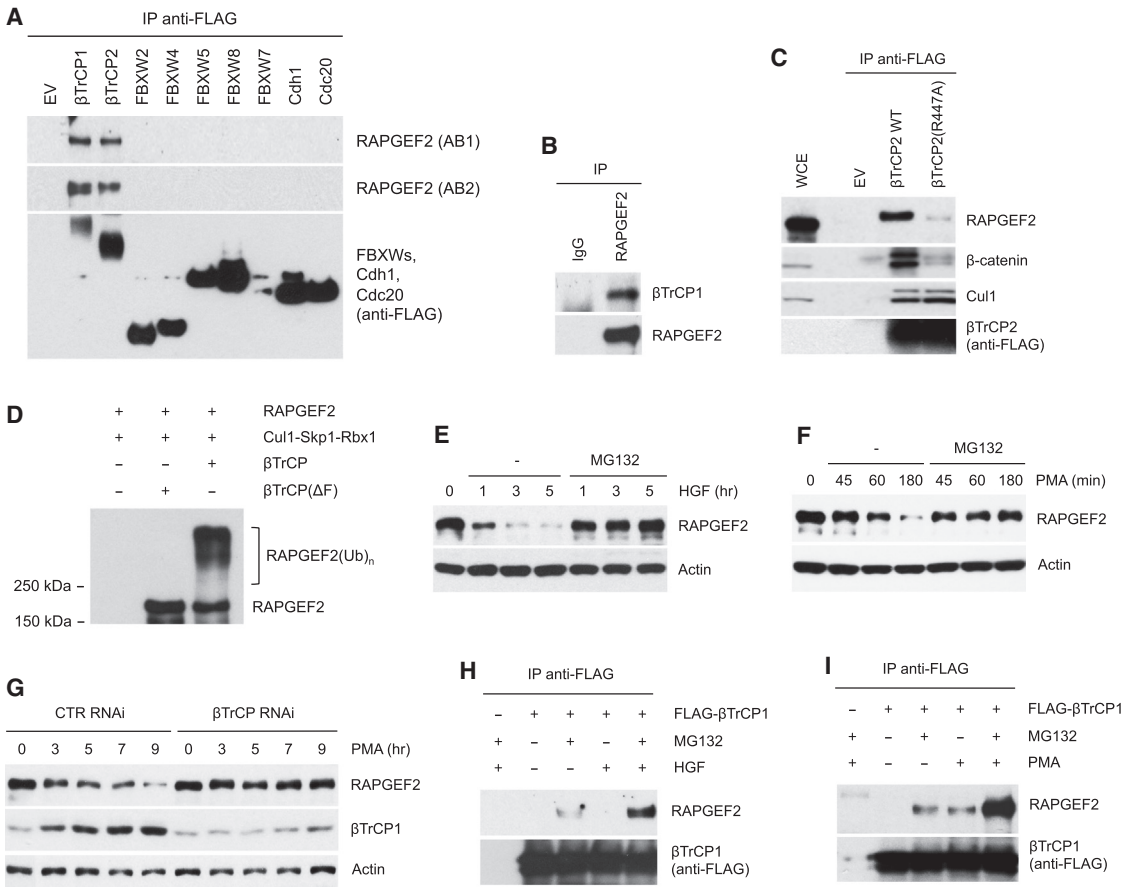

Figure 1. RAPGEF2 Is Targeted for Degradation by SCF$^{\beta TrCP}$ in Response to Stimuli that Induce Cell Migration

(A) The indicated FLAG-tagged F-box proteins (FBPs), the APC/C activators Cdh1 and Cdc20 or an empty vector (EV) were expressed in HEK293T cells. Forty-eight hours after transfection, cells were treated for 5 hr with the proteasome inhibitor MG132, then harvested and lysed. Whole cell extracts were immunoprecipitated (IP) with anti-FLAG resin and immunoblotted with the indicated antibodies. AB1 and AB2 are two different anti-RAPGEF2 antibodies.

(B) HEK293T cells were treated for 5 hr with the proteasome inhibitor MG132, then harvested and lysed. Whole cell extracts were immunoprecipitated (IP) with anti-RAPGEF2 antibody and immunoblotted with the indicated antibodies.

(C) Arg447 in the WD40 repeat of βTrCP2 is required for the interaction with RAPGEF2. HEK293T cells were transfected as indicated and analyzed as in (A). WCE, whole cell extract; WT, wild-type.

(D) RAPGEF2, Skp1, Cul1, and Rbx1 were expressed in HEK293T cells in the absence or presence of FLAG-tagged βTrCP1 or a FLAG-tagged βTrCP1(ΔF-box) mutant. After immunopurification with anti-FLAG resin, in vitro ubiquitylation of RAPGEF2 was performed as described in the Supplemental Experimental Procedures. Samples were analyzed by immunoblotting with an anti-RAPGEF2 antibody. The bracket indicates a ladder of bands corresponding to poly-ubiquitylated RAPGEF2.

(E and F) MDCK cells were treated with HGF (E) or PMA (F) with or without the proteasome inhibitor MG132. Cells were collected at the indicated times and lysed. Whole cell extracts were subjected to immunoblotting with the indicated antibodies. Actin is shown as a loading control.

(G) HEK293 cells were transfected with the indicated siRNA oligonucleotides and treated with PMA. Cells were then collected and analyzed as in (E).

(H and I) HEK293 cells were transfected with an empty vector or FLAG-tagged βTrCP1. Forty-eight hours after transfection, cells were treated, when indicated, with MG132 and with either HGF (H) or PMA (I) for 4 hr, then harvested and lysed. Whole cell extracts were immunoprecipitated (IP) with anti-FLAG resin, and immunoblotted with anti-RAPGEF2 and anti-FLAG antibodies.

See also Figure S1.

and have an intact HGF signaling (Sakkab et al., 2000). The degradation of RAPGEF2 in response to the motogenic stimulus is a rapid event that starts much earlier than the downregulation of E-cadherin, suggesting that the degradation of RAPGEF2 is not an indirect consequence of cell junction disassembly (data not shown).

To test whether the degradation of RAPGEF2 observed in response to factors that induce cell migration is mediated by βTrCP, we reduced the levels of both βTrCP1 and βTrCP2 in HEK293 cells using a previously validated siRNA (Guardavaccaro et al., 2008; Kruiswijk et al., 2012). We found that βTrCP knockdown blocked the PMA-induced degradation of RAPGEF2 (Figure 1G). Accordingly, the binding of βTrCP to endogenous RAPGEF2 was stimulated by both HGF and PMA (Figures 1H and 1I).

HGF-Induced Phosphorylation of RAPGEF2 by CK1α Triggers RAPGEF2 Degradation

The WD40 β-propeller structure of βTrCP interacts with its substrate proteins via a diphosphorylated degradation motif

(phosphodegron) with the consensus DpSGXX(X)pS (Cardozo and Pagano, 2004; Frescas and Pagano, 2008; Wu et al., 2003). We identified one canonical DpSGXX(X)pS motif in human RAPGEF2 that might potentially be the phosphodegron (Figure S2A). We mutated the serine residues in this motif to alanine and determined the ability of the RAPGEF2 mutant to interact with βTrCP. Whereas wild-type RAPGEF2 immunoprecipitated βTrCP1, the RAPGEF2(S1244A/S1248A) mutant did not (Figure 2A). The motif surrounding S1244 and S1248 is highly conserved in vertebrate orthologs of RAPGEF2 (Figure 2B).

As a further method to examine whether phosphorylation is required for the interaction of RAPGEF2 with βTrCP, we used immobilized synthetic peptides comprising the βTrCP-binding domain of RAPGEF2 (aa 1240–1252 in human RAPGEF2). As shown in Figure 2C, a RAPGEF2-derived peptide containing phosphoserine residues at positions Ser1244 and Ser1248 associated with in vitro translated βTrCP1, but not with a different F-box protein, whereas the unphosphorylated peptide did not associate at all, suggesting that phosphorylation of Ser1244 and Ser1248 directly mediates the association with βTrCP.

To investigate whether Ser1244 and Ser1248 are phosphorylated in vivo in response to factors that induce cell motility, we generated a phosphospecific antibody against the ^{1240}DAADpSGRGpSWTSC^{1252} peptide with phosphoserine residues at positions 1244 and 1248. This antibody detected wild-type RAPGEF2, but not the RAPGEF2(S1244A/S1248A) mutant (Figure S2B). Moreover, λ-phosphatase treatment of immunoprecipitated wild-type RAPGEF2 inhibited RAPGEF2 detection by the phosphospecific antibody (Figure S2C). We then used this antibody to test whether RAPGEF2 is phosphorylated in vivo. Figure 2D shows that RAPGEF2 was phosphorylated on Ser1244 and Ser1248 in HEK293 cells that were treated with HGF.

In the RAPGEF2 immunopurification described above, we also recovered three peptides corresponding to casein kinase 1 (CK1, isoform α; Figure S2D). We first confirmed that CK1α coimmunoprecipitated with RAPGEF2 in vivo (Figure S2E). To test whether CK1α is involved in the phosphorylation of RAPGEF2, we used pharmacological inhibitors and found that the CK1 inhibitors D4476 and IC261 prevented both the HGF-induced binding of βTrCP1 to RAPGEF2 and the phosphorylation of RAPGEF2 on Ser1244/Ser1248 (Figure 2E). Accordingly, D4476 blocked the HGF-induced degradation of RAPGEF2 (Figure 2F). To rule out nonspecific effects of these inhibitors, we silenced CK1α by RNAi (Gao et al., 2011; Tapia et al., 2006). The knockdown of CK1α inhibited the proteasome-dependent degradation of RAPGEF2 in response to HGF (Figure 2G) as well as RAPGEF2 interaction with βTrCP (Figure 2H).

In order to determine if CK1α directly phosphorylates the RAPGEF2 degron, we carried out an in vitro kinase assay, using purified recombinant CK1α. CK1α, but not CK2, GSK3β, or CDK1 (kinases involved in the phosphorylation of other substrates of βTrCP), phosphorylated the degron of RAPGEF2 in vitro, as shown by the recognition by our phosphospecific antibody (Figure 2I). Altogether these results indicate that CK1α-mediated phosphorylation of RAPGEF2 on Ser1244/Ser1248 is required for RAPGEF2 degradation induced by HGF.

IKKβ-Mediated Phosphorylation of RAPGEF2 Is Required for RAPGEF2 Degradation

Substrates of βTrCP are phosphorylated on their degrons following an initial phosphorylation event that either generates a binding site for the kinase phosphorylating the degron or exposes an otherwise masked degron. We noticed a consensus sequence for phosphorylation by I-kappa-B kinase (IKK) in close proximity to the RAPGEF2 phosphodegron (Figure S3A). Phorbol esters (PMA) and HGF have been shown to stimulate the activity of IKKβ in epithelial cells (Fan et al., 2005, 2007, 2009; Hah and Lee, 2003; Huang et al., 2003; Müller et al., 2002). First, we confirmed that treatment of epithelial cells with HGF or PMA results in the activation of IKKβ (Figure S3B). We then tested whether IKKβ is able to phosphorylate RAPGEF2 by performing an in vitro kinase assay using recombinant kinases and immunopurified RAPGEF2, which had been previously dephosphorylated. IKKβ, and to a lesser extent IKKα, were able to phosphorylate RAPGEF2 (as shown by incorporation of radiolabeled phosphate), however, no phosphorylation was detected by our phosphospecific antibody on the RAPGEF2 degron (Figures 3A and S3C), indicating that IKKα/β phosphorylates residues of RAPGEF2 different from Ser1244 and Ser1248.

Next, we tested whether RAPGEF2 phosphorylation by IKKβ affects the CK1α-dependent phosphorylation of the RAPGEF2 degron in vitro. When purified recombinant IKKβ was used to phosphorylate RAPGEF2 (and washed away before CK1α addition), stimulation of the CK1α-mediated phosphorylation of the RAPGEF2 degron was observed (Figures 3B and S3C). IKKα did not have any effect on the CK1α-mediated phosphorylation of the RAPGEF2 degron (Figure S3C). Accordingly, in cultured cells, CK1α-mediated phosphorylation of the RAPGEF2 degron (Figures 3C and 3D), RAPGEF2 binding to βTrCP (Figure 3D), and RAPGEF2 ubiquitylation (Figure 3E) were stimulated by the overexpression of wild-type IKKβ and, more extensively, the constitutively active IKKβ(S177E/S181E) mutant.

To assess whether IKKβ is involved in the degradation of RAPGEF2, we overexpressed IKKβ and analyzed the abundance of RAPGEF2 in the absence or presence of the proteasome inhibitor MG132. Overexpression of the constitutively active IKKβ(S177E/S181E) mutant, but not the constitutively inactive IKKβ(S177A/S181A) mutant, resulted in RAPGEF2 downregulation, which was prevented by proteasomal inhibition (Figure 3F). Conversely, knockdown of IKKβ prevented both the HGF- and the PMA-induced degradation of RAPGEF2 (Figures 3G, 3H, and S3D). Accordingly, pharmacological inhibition of IKK blocked both the CK1α-dependent phosphorylation of the RAPGEF2 degron and RAPGEF2 binding to βTrCP (Figure 3I). Further, we found that IKKβ was coimmunoprecipitated with RAPGEF2 in vivo (Figure S3E). Taken together, these results indicate that IKKβ-dependent phosphorylation of RAPGEF2 is required for RAPGEF2 degradation induced by HGF and mediated by βTrCP.

We then employed mass spectrometry to pinpoint the specific RAPGEF2 sites targeted by IKKβ. Immunopurified, dephosphorylated RAPGEF2 was subjected to an in vitro kinase assay in the presence or absence of purified kinases, prior to mass spectrometry analysis. We identified phosphopeptides containing phospho-Ser1254 in IKKβ-treated RAPGEF2 samples (Figures S3F and S3G). These phosphopeptides were not found in

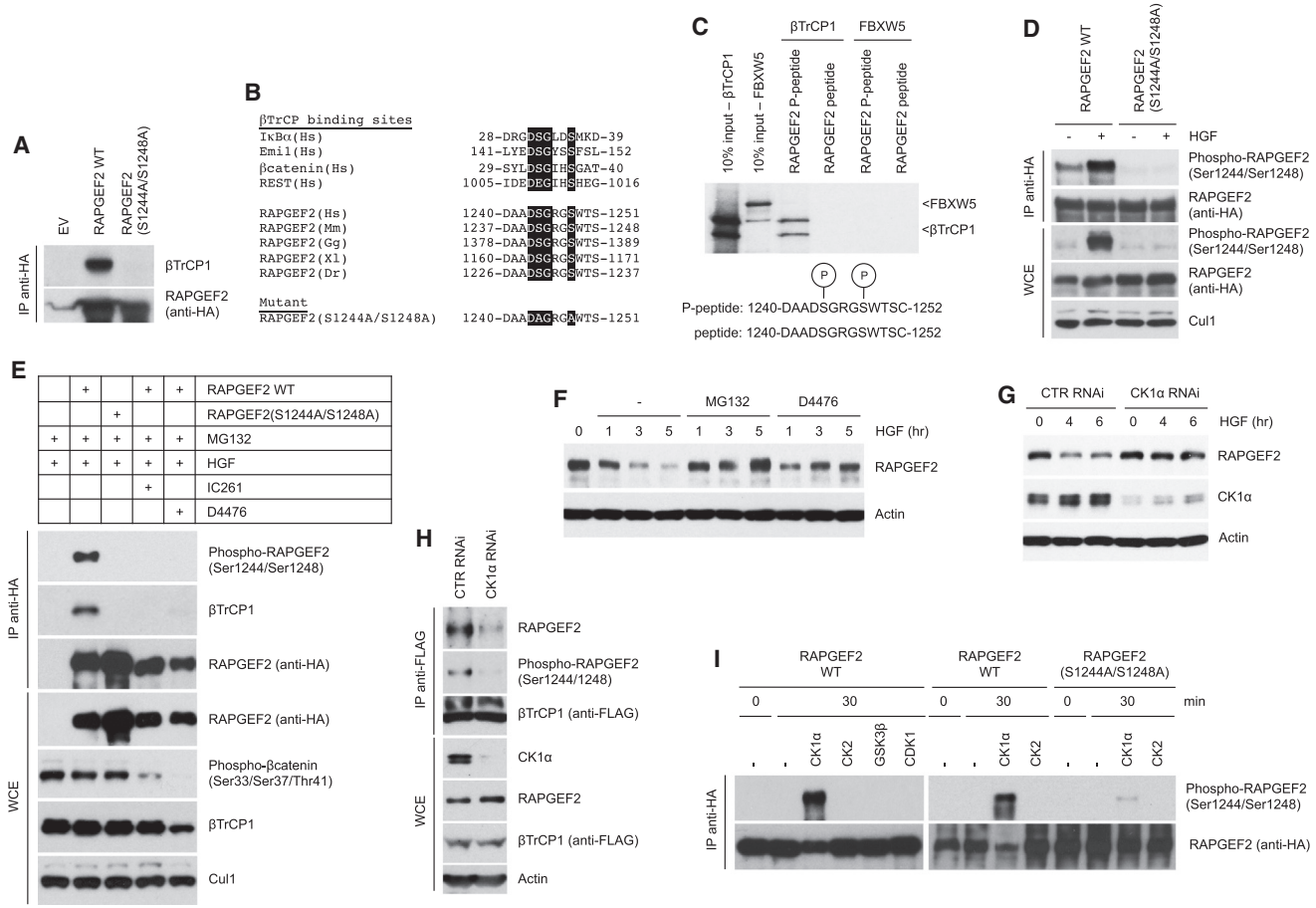

Figure 2. CK1α-Dependent Phosphorylation of RAPGEF2 Is Required for Its Degradation

(A) HEK293T cells were transfected with an empty vector (EV), HA-tagged wild-type RAPGEF2, or HA-tagged RAPGEF2(S1244A/S1248A). Forty-eight hours after transfection, cells were harvested and lysed. Whole cell extracts were subjected to immunoprecipitation (IP) with anti-HA resin, followed by immunoblotting with the indicated antibodies.

(B) Alignment of the amino acid regions corresponding to the βTrCP-binding motif in RAPGEF2 orthologs and previously reported βTrCP substrates (top). Schematic representation of Ser to Ala substitutions in the βTrCP-binding motif of RAPGEF2. The amino acidic sequence of the double mutant is shown (bottom).

(C) Ser1244 and Ser1248 in RAPGEF2 require phosphorylation to bind βTrCP1. ^{35}S-βTrCP1 and ^{35}S-FBXW5 were transcribed/translated in vitro and incubated with beads coupled to peptides spanning the RAPGEF2 degron (unphosphorylated or phosphorylated). Beads were washed with Triton X-100 buffer and bound proteins were eluted and subjected to electrophoresis and autoradiography. The first two lanes correspond to 10% of the in vitro translated protein inputs. Peptide sequence spanning the RAPGEF2 degron is shown in the bottom panel.

(D) HEK293 cells expressing HA-tagged wild-type RAPGEF2 were treated with the proteasome inhibitor MG132 in the presence of absence of HGF. Cells were collected and lysed. Whole cell extracts were subjected to direct immunoblotting with the indicated antibodies or immunoprecipitation with anti-HA resin followed by immunoblotting with the indicated antibodies. Cul1 is shown as a loading control.

(E) HEK293 cells were transfected with HA-tagged wild-type RAPGEF2 or HA-tagged RAPGEF2(S1244A/S1248A). Forty-eight hours after transfection, cells were treated with HGF and MG132 for 4 hr in the presence of absence of the indicated kinase inhibitors. Cells were then harvested and lysed. Whole cell extracts were immunoprecipitated (IP) with anti-HA resin and analyzed by immunoblotting.

(F) MDCK cells were treated with HGF and the indicated compounds. Cells were lysed and collected. Whole cell extracts were then immunoblotted with the indicated antibodies. Actin is shown as a loading control.

(G) HEK293 cells were transduced with the indicated lentiviral shRNA vectors. Cells were then treated with HGF for the indicated times. Cells were collected and lysed. Whole cell extracts were treated as in (F).

(H) HEK293 cells, treated as in (G), were transfected with FLAG-tagged βTrCP1. Cells were treated with HGF and MG132 for 4 hr. Cells were then harvested and lysed. Whole cell extracts were immunoprecipitated (IP) with anti-FLAG resin, and analyzed by immunoblotting.

(I) The RAPGEF2 degron is phosphorylated by CK1α in vitro. Immunopurified wild-type RAPGEF2 or RAPGEF2(S1244A/S1248A) were first dephosphorylated by treatment with lambda phosphatase and then incubated with the indicated purified kinases in the presence of ATP. Reactions were stopped by adding Laemmli buffer and analyzed by immunoblotting.

See also Figure S2.

RAPGEF2 treated with other kinases (RSK1, CK1α, CK2) or when no kinase was added to the assay. Mutation of Ser1254 to Ala in RAPGEF2 inhibited (1) CK1α-dependent phosphorylation of the RAPGEF2 degron (Figure 3J, middle panel), (2) RAPGEF2 interaction with βTrCP (Figure 3J, top panel), and (3) RAPGEF2 turnover (Figure S3H). Altogether, results indicate that

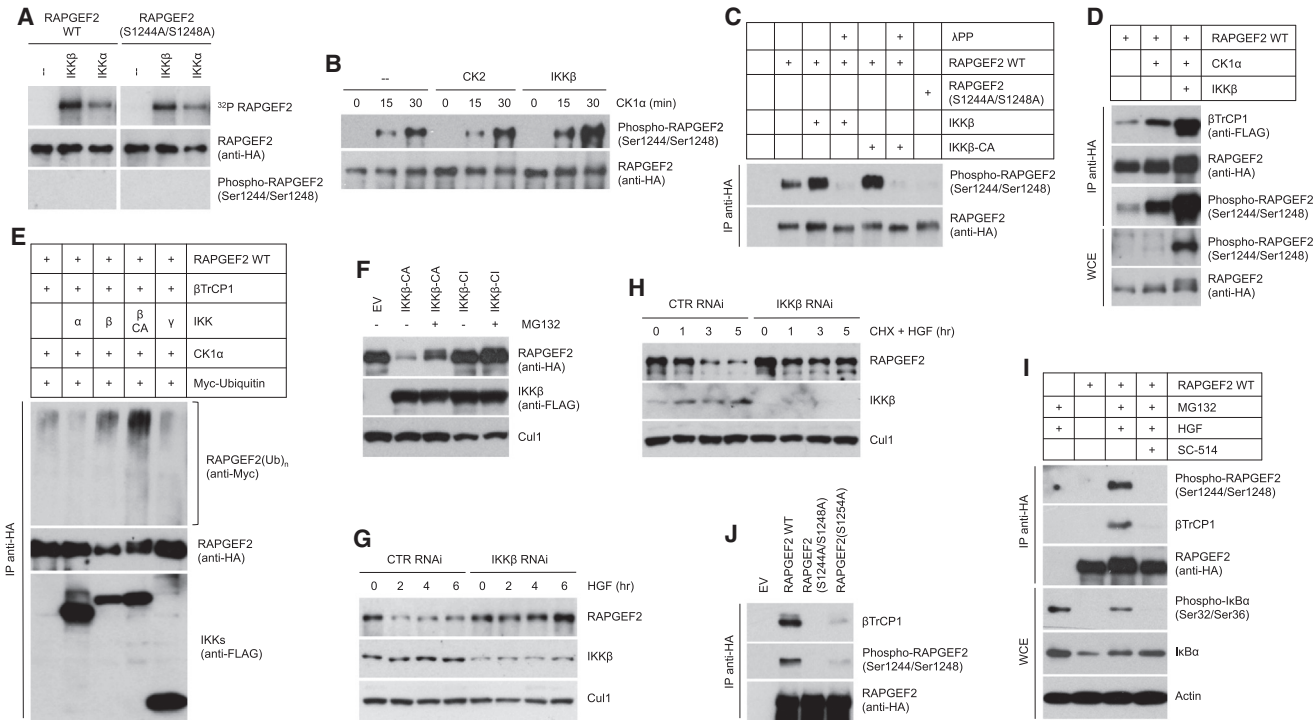

Figure 3. IKKβ Stimulates the CK1α-Mediated Degradation of RAPGEF2

(A) Immunopurified wild-type RAPGEF2 and RAPGEF2(S1244A/S1248A) were first dephosphorylated by treatment with lambda phosphatase and then incubated with the indicated purified kinases in the presence of γ^{32}P ATP. Reactions were stopped by adding Laemmli buffer, run on SDS-PAGE and analyzed by autoradiography (top panels) and immunoblotting (bottom panels).

(B) Immunopurified wild-type RAPGEF2 was first dephosphorylated by treatment with lambda phosphatase and then incubated with the indicated kinases. Kinases were then washed away prior to addition of CK1α. Reactions were stopped at the indicated times and analyzed by immunoblotting.

(C and D) HEK293 cells were transfected with the indicated constructs. Cells were treated with HGF and MG132 for 4 hr. Cells were then harvested and lysed. Whole cell extracts were immunoprecipitated (IP) with anti-HA resin, and immunoblotted with antibodies specific for the indicated proteins. Immunocomplexes were treated with lambda phosphatase when indicated. CA, constitutively active.

(E) HEK293 cells, transfected with the indicated constructs, were treated as in (C), then harvested and lysed in 0.1% Triton X-100 lysis buffer. Whole cell extracts were denatured by adding 1% SDS and boiling for 10 min. SDS was quenched and diluted. Whole cell extracts were then immunoprecipitated (IP) with anti-HA resin, and immunoblotted with antibodies specific for the indicated proteins. The bracket indicates a ladder of bands corresponding to poly-ubiquitylated RAPGEF2.

(F) HEK293 were transfected with HA-tagged RAPGEF2 and the constitutively active IKKβ(S177E/S181E) or inactive IKKβ(S177A/S181A) mutant and treated with MG132 in presence of HGF. After 48 hr, cells were collected, lysed and subjected to immunoblotting. CA, constitutively active; CI, constitutively inactive.

(G and H) Cells were transfected with the indicated siRNA oligonucleotides and treated with HGF only (G) or HGF and cycloheximide (H) to block protein synthesis. Cells were then collected at the indicated times. Whole cell extracts were analyzed by immunoblotting. Cul1 is shown as a loading control.

(I) HEK293 cells were transfected with HA-tagged wild-type RAPGEF2. Forty-eight hours after transfection, cells were treated with HGF and MG132 for 4 hr in the presence or absence of the IKK inhibitor SC-514. Cells were then harvested and lysed. Whole cell extracts were immunoprecipitated (IP) with anti-HA resin, and immunoblotted with the indicated antibodies.

(J) HEK293 cells were transfected with an empty vector (EV), HA-tagged wild-type RAPGEF2, HA-tagged RAPGEF2(S1244A/S1248A), or HA-tagged RAPGEF2(S1254A). Forty-eight hours after transfection, cells were treated with the proteasome inhibitor MG132 in the presence of HGF, then harvested and lysed. Whole cell extracts were analyzed as in (I).

See also Figure S3.

IKKβ-mediated phosphorylation of RAPGEF2 on Ser1254 promotes the phosphorylation of the RAPGEF2 degron by CK1α, RAPGEF2 binding to βTrCP, and RAPGEF2 degradation.

RAPGEF2 Degradation Controls the HGF-Induced Migration of Epithelial Cells

To examine the biological function of RAPGEF2 degradation, we transduced MDCK cells with lentiviruses expressing physiological levels of wild-type RAPGEF2 or RAPGEF2(S1244A/S1248A) (Figure S4A). We first confirmed that both the steady state levels and the half-life of RAPGEF2(S1244A/S1248A) were increased when compared with wild-type RAPGEF2 in MDCK cells treated with HGF (Figures 4A and 4B) or PMA (Figures S4B and S4C). As expected, growth factors that do not induce scattering of MDCK cells, such as EGF and PDGF, did not lead to degradation of either wild-type RAPGEF2 or RAPGEF2(S1244A/S1248A) (Figures S4D and S4E). Notably, the RAPGEF2(S1244A/S1248A) mutant that escaped degradation upon HGF stimulation localized to the plasma membrane (Figure S4F).

Next, we examined whether RAPGEF2 degradation affected the activity of Rap1 in response to HGF. Whereas in cells

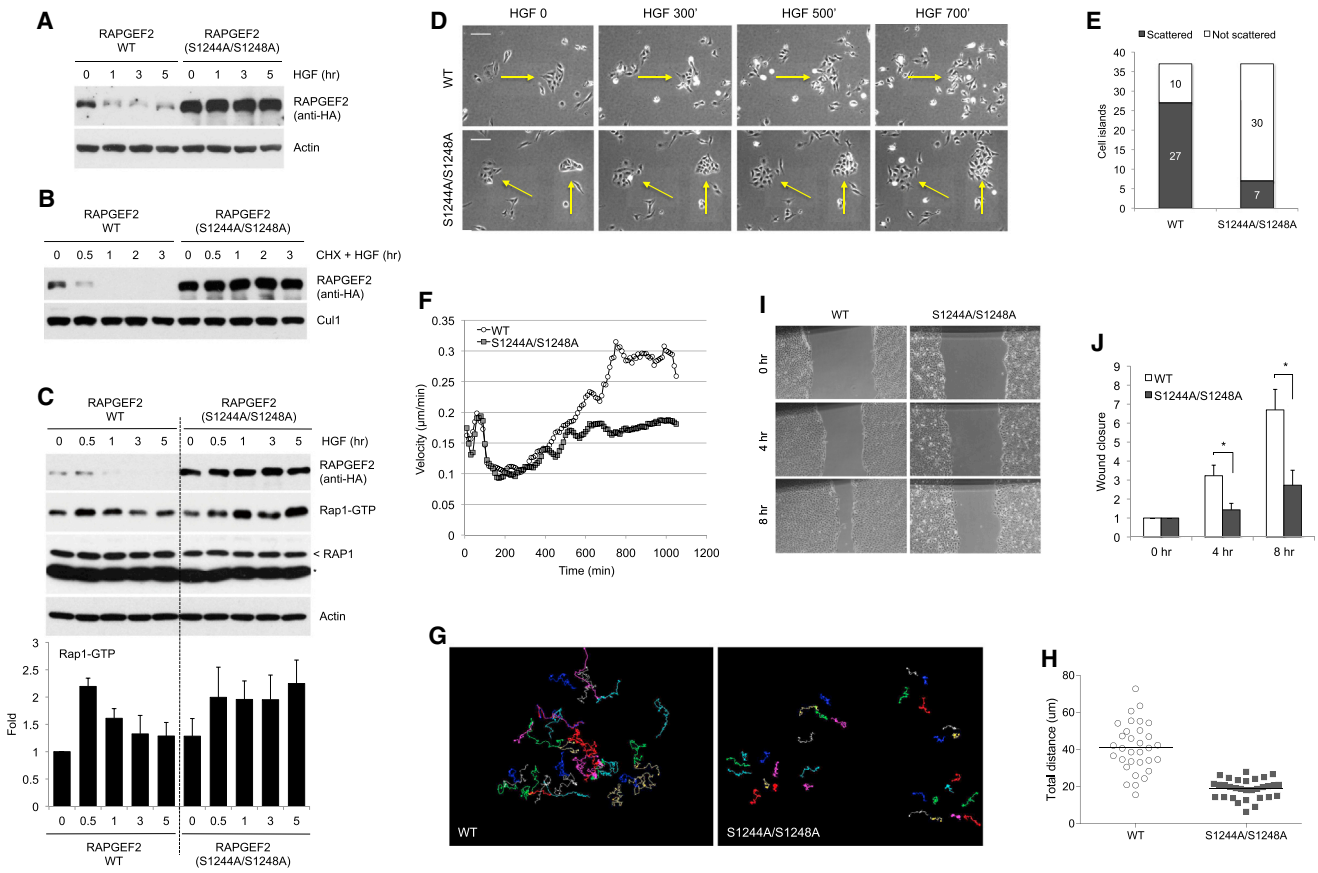

Figure 4. RAPGEF2 Degradation Is Required for Rap1 Inactivation and Stimulation of Cell Migration in Response to HGF

(A and B) MDCK cells, transduced with lentiviruses expressing HA-tagged wild-type RAPGEF2 or HA-tagged RAPGEF2(S1244A/S1248A), were treated with HGF only (A) or HGF and the inhibitor of protein synthesis cycloheximide (B) for the indicated times. Cells were then collected and analyzed by immunoblotting. Actin and Cul1 are shown as a loading control.

(C) MDCK cells, transduced as in (A), were treated with HGF for the indicated times. Cells were collected and lysed. Whole cell extracts were analyzed by immunoblotting with the indicated antibodies and in a pull-down assay using a GST fusion of the activated Rap1-binding domain of RalGDS. The levels of precipitated Rap1 were determined by immunoblotting using an anti-Rap1 antibody. The asterisk indicates a nonspecific band. Actin is shown as a loading control. To facilitate comparison, a dotted line separates samples from cells expressing wild-type RAPGEF2 and samples from cells expressing RAPGEF2(S1244A/S1248A). The graph shows the abundance of Rap1-GTP normalized to total Rap1 and relative to Rap1-GTP in cells expressing wild-type RAPGEF2 at time 0. Values are averaged with the ones from three additional independent experiments (n = 4 ± SD).

(D) MDCK cells, transduced with lentiviruses expressing wild-type RAPGEF2 or RAPGEF2(S1244A/S1248A), were treated with HGF and imaged by time-lapse phase-contrast microscopy for 16 hr. Representative phase-contrast images from the time-lapse series are shown. Scale bars represent 100 μm.

(E) Quantification of scattering from time-lapse experiments. The graph shows the number of islands scattered (islands in which cells have disrupted cell-cell contacts) after HGF treatment. $p < 0.001$ (Pearson's χ^2 test). Only islands including 5–15 cells were scored.

(F) An automated cell tracking software was employed to measure the average migration velocity of MDCK cells expressing wild-type RAPGEF2 or the RAPGEF2(S1244A/S1248A) mutant in the presence of HGF. For each cell line/condition, three independent time-lapse image series (at least 300 individual cells) were analyzed.

(G) Representative individual migratory tracks of MDCK cells expressing wild-type RAPGEF2 or RAPGEF2(S1244A/S1248A) in the presence of HGF.

(H) Track distance of individual cells shown in (G). Horizontal lines represent the mean. $p < 0.001$ (Student's t test).

(I) MDCK cells expressing wild-type RAPGEF2 or the RAPGEF2(S1244A/S1248A) mutant were grown to confluence. Cell monolayers were wounded and then treated with HGF. Cells were photographed immediately after wounding (0 hr) and after 4 (4 hr) and 8 hr (8 hr).

(J) The graph represents the relative wound closure at 0, 4, and 8 hr (n = 5 ± SD).

*p = 0.005 (Student's t test). See also Figure S4.

expressing wild-type RAPGEF2, Rap1 was first rapidly activated and then inactivated following HGF treatment (as shown by the amount of the GTP-bound Rap1), cells expressing the stable RAPGEF2 mutant displayed sustained Rap1 activity (Figure 4C). On the contrary, Rap2 activity was neither regulated by HGF treatment nor affected by RAPGEF2 degradation in HGF-treated cells (data not shown).

To assess the effect of defective degradation of RAPGEF2 on HGF-induced cell scattering, we employed a live-cell microscopy assay (de Rooij et al., 2005; Loerke et al., 2012). MDCK cells expressing physiological levels of wild-type RAPGEF2 or RAPGEF2(S1244A/S1248A) were treated with HGF and followed by time-lapse imaging (Figure 4D). We quantified cell scattering by scoring the percentage of cell islands (groups of 5–16 cells) in

which three or more cells had disrupted contacts with neighboring cells (Figure 4E). MDCK cells expressing the stable RAPGEF2(S1244A/S1248A) mutant displayed decreased scattering when compared with cells expressing wild-type RAPGEF2. Next, we employed an automated cell tracking software that tracks individual cell velocity and trajectories from consecutive time-lapse images (de Rooij et al., 2005; Loerke et al., 2012). As shown in Figure 4F, cells expressing the RAPGEF2 stable mutant displayed defective induction of average cell speed following HGF treatment. Accordingly, individual migratory tracks of MDCK cells expressing RAPGEF2(S1244AS1248A) treated with HGF were shorter when compared with the ones of MDCK cells expressing wild-type RAPGEF2 (Figures 4G and 4H).

Scattering of epithelial cells in response to HGF is characterized by two major steps, i.e., loss of cell adhesion, followed by an increase in cell motility (Loerke et al., 2012). To assess in which of these two processes the degradation of RAPGEF2 is involved, we analyzed the motility of noncontacted cells (not starting from cell islands) expressing wild-type RAPGEF2 or the nondegradable RAPGEF2(S1244A/S1248A) mutant in response to HGF. As shown in Figures S4G–S4I, HGF-induced motility of noncontacted cells expressing RAPGEF2(S1244A/S1248A) is reduced when compared with the one of noncontacted cells expressing wild-type RAPGEF2 indicating that the degradation of RAPGEF2 is required for the HGF-induced increase in cell migration even in the absence of adherens junctions.

To confirm that the nondegradable RAPGEF2 mutant inhibits cell motility independently of cell-cell adhesion, we analyzed the HGF-induced scattering in cells in which cell-cell junctions were previously inhibited by low calcium conditions (Figures S4J–S4M). Cells expressing the stable RAPGEF2 mutant displayed a remarkable decrease in motility when compared with cells expressing wild-type RAPGEF2 even in low calcium conditions.

Taken together, these results indicate that RAPGEF2 degradation is required for HGF-induced cell migration. As expected, HGF-induced motility of MDCK cells was inhibited if RAPGEF2 degradation was bypassed by ectopic expression of the constitutively active Rap1V12 mutant (Figures S4N–S4O).

As an additional method to analyze the role of RAPGEF2 degradation in cell migration, we employed the wound-healing assay, which monitors the HGF-stimulated migration of cells into a scratch made in a confluent monolayer of MDCK cells. Following treatment with HGF, MDCK cells expressing the nondegradable RAPGEF2(S1244A/S1248A) mutant were unable to close the wound gap (Figures 4I and 4J).

Many studies have demonstrated that Rap1 controls inside-out signaling regulating integrin activity (Arai et al., 2001; Bos et al., 2001; Caron et al., 2000; Katagiri et al., 2000, 2003; Kinbara et al., 2003; Reedquist et al., 2000; Sebzda et al., 2002). To test whether the defective migration of MDCK cells expressing the degradation-resistant RAPGEF2 mutant is linked to misregulation of integrin activity, we analyzed the activity of β1-integrins in HGF-treated MDCK cells using an antibody (9EG7) that detects the active conformation of β1-integrins. As shown in Figures S4P and S4Q, untreated MDCK cells expressing either wild-type RAPGEF2 or RAPGEF2(S1244A/S1248A) displayed 9EG7 staining mostly at the cell periphery. Whereas HGF treatment of cells expressing wild-type RAPGEF2 resulted in a general reduction of 9EG7 staining, it did not cause any detectable change in the intensity of 9EG7 staining in MDCK cells expressing the degradation-resistant RAPGEF2 mutant. Of note, the expression of β1-integrins did not change in response to HGF either in control cells or in cells expressing the RAPGEF2(S1244A/S1248A) mutant (data not shown). These results indicate that in cells expressing the degradation-resistant RAPGEF2 mutant, defective stimulation of cell motility correlates with misregulation of β1-integrins activity.

Failure to Degrade RAPGEF2 Inhibits Invasion and Metastasis of Human Breast Cancer Cells

Next, we investigated the role of the CK1α-IKKβ-βTrCP-mediated degradation of RAPGEF2 in mediating tumor cell invasion, dissemination, and metastasis. Highly metastatic MDA-MB-231 breast cancer cells expressing physiological levels of wild-type RAPGEF2 or RAPGEF2(S1244A/S1248A) were assayed for their invasion potential in vitro using a standard transwell assay. As shown in Figures 5A–5C, expression of the degradation-resistant RAPGEF2(S1244A/S1248A) mutant greatly inhibited the invasive migration of MDA-MB-231 cells stimulated by HGF.

We then tested the metastatic potential of MDA-MB-231 breast cancer cells expressing the degradation-resistant RAPGEF2 mutant using a zebrafish xenograft model for cancer invasion-metastasis (Lee et al., 2009; Zhang et al., 2012). We injected red-fluorescent-labeled MDA-MB-231 cells expressing physiological levels of wild-type RAPGEF2 or RAPGEF2(S1244A/S1248A) into the perivitelline space (ventrally from the sub intestinal vein and anterior from the Duct of Cuvier) of 48-hpf zebrafish embryos bearing green-fluorescent-labeled endothelial cells [*Tg(fli1a:eGFP)*] (Figure 5D). Tumor cell dissemination was examined in the trunk region 48 hr postinjection. Strikingly, cells expressing wild-type RAPGEF2 (as well as parental MDA-MB-231 cells) disseminated to the trunk region, whereas cells expressing the nondegradable RAPGEF2 mutant displayed a remarkably decreased ability to disseminate and metastasize (Figures 5E–5G). Of note, neither the rate and amount of neovascularization nor the tumor size of the xenografts showed apparent difference between the conditions.

DISCUSSION

In this study, we demonstrate that when cells are stimulated with factors that induce cell motility, such as the metastatic factor HGF, the Rap guanine nucleotide exchange factor RAPGEF2 is rapidly targeted for proteasome-dependent degradation by the $SCF^{\beta TrCP}$ ubiquitin ligase in cooperation with IKKβ and CK1α. By phosphorylating RAPGEF2 on Ser1254, IKKβ primes RAPGEF2 for phosphorylation by CK1α on a conserved degron (Ser1244/Ser1248) triggering RAPGEF2 ubiquitylation and proteasomal degradation.

These findings reveal a molecular mechanism by which HGF-MET signaling, which can be induced through paracrine and autocrine production of HGF, stimulates epithelial cell motility. By triggering the destruction of RAPGEF2, HGF induces the inactivation of Rap1, a crucial regulator of the integrin function.

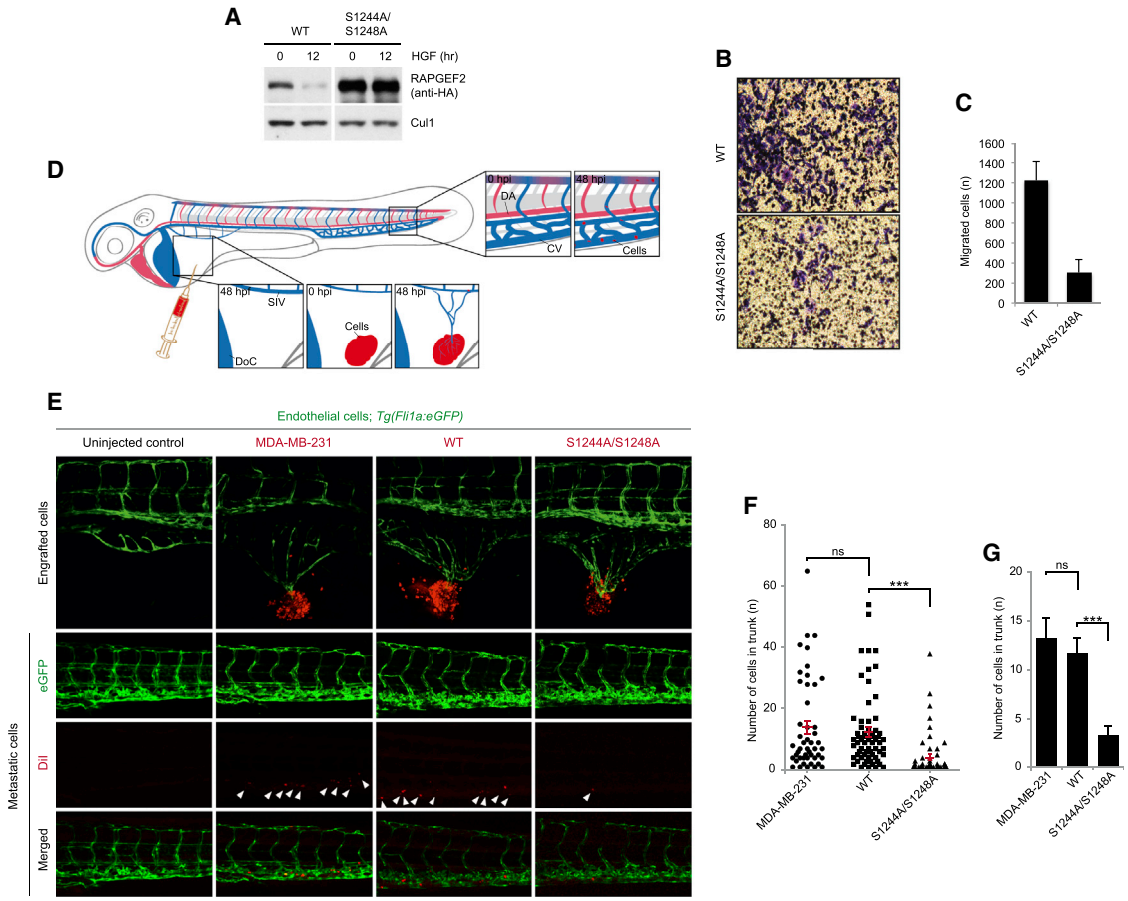

Figure 5. Expression of a Degradation-Resistant RAPGEF2 Mutant Blocks Invasion and Metastasis of Human Breast Cancer Cells

(A) MDA-MB-231 breast cancer cells, transduced with lentiviruses expressing HA-tagged wild-type RAPGEF2 or HA-tagged RAPGEF2(S1244A/S1248A), were treated with HGF for the indicated times. Cells were then collected and analyzed by immunoblotting with the indicated antibodies. Cul1 is shown as a loading control.

(B and C) MDA-MB-231 cells, transduced as in (A), were subjected to an in vitro invasion assay using HGF as chemoattractant as described in Supplemental Experimental Procedures. Invading cells were stained with crystal violet. Representative photographs of three experiments are shown in (B). Quantification of cells that invaded through the matrix is shown in (C). Data are mean ± SD of three experiments.

(D) Scheme of the zebrafish embryo and injections performed.

(E) MDA-MB-231 breast cancer cells expressing wild-type RAPGEF2 or RAPGEF2(S1244A/S1248A) were labeled with DiI and injected into the perivitelline space of 48-hpf *Tg(fli1a:eGFP)* zebrafish embryos. Parental MDA-MB-321 cells were used as additional control. Dissemination of cancer cells were scored in the trunk region 2 days postinjection using confocal microscopy. Representative micrographs of tumor and neovascularization (upper panel) and trunk region with metastatic cells (lower panels) 48 hr postinjection are shown.

(F and G) The graphs show the quantification of the number of cells metastasized to the trunk region (at least n = 50 injections for each condition). Data are presented as the average (±SEM) compared to the control condition from two independent experiments. For statistical analysis Kruskal-Wallis test was used with Dunn's post hoc test (***$p < 0.001$).

Failure to degrade RAPGEF2 in response to HGF results in sustained Rap1 and integrin activity and prevents the HGF-induced stimulation of epithelial cell migration.

A number of studies have reported seemingly contradictory results on the role of Rap1 in the regulation of cell migration. Indeed, it has been shown that either increased or decreased activity of Rap1 promotes cell motility (Ahmed et al., 2012; Freeman et al., 2010; Kim et al., 2012; Lyle et al., 2008; McSherry et al., 2011; Ohba et al., 2001; Yajnik et al., 2003; Zheng et al., 2009). Moreover, in cancer cells, both overactivation and inactivation of Rap1 have been associated with increased metastasis. These conflicting findings can be explained at least in part by cell type-specific and tumor type-specific effects of Rap1 on cell migration and invasiveness. Indeed, it has been reported that activated Rap1 promotes the metastatic invasion of prostate and pancreatic carcinoma cells but inhibits invasion of osteosarcoma and squamous cell carcinoma cells.

Interestingly, preventing Rap1 activation (by ectopic expression of Rap1GAP) or cycling (by expressing a constitutively active Rap1 mutant) inhibits the ability of melanoma cells to extravasate from the microvasculature and form metastatic lesions in the lungs, indicating that dynamic regulation of Rap1 activity is required for metastatic dissemination of melanoma cells (Freeman et al., 2010). It is also important to mention that various means, e.g., overexpression/activation of different Rap1 GEFs or GAPs, overexpression of constitutively active, or

inactive Rap1 mutants, have been employed to manipulate the activity of Rap1. These different strategies can affect distinct cellular pools of Rap1, which, via different Rap1 effectors, can lead to different outcomes. Furthermore, it is well established that Rap1 controls multiple steps in the metastatic cascade, from the initial movement through the stroma and the intravasation into the blood and lymphatic vessels, to the extravasation and invasion of the stroma of a second tumor site. As a result, whereas a specific step might require activation of the Rap1-integrin signaling and increased cell adhesion to the extracellular matrix, a different step might benefit from decreased Rap1/integrin activity and decreased adhesion. In this regard, during HGF-induced cell scattering, we observe a biphasic regulation of Rap1 with an initial rapid increase of Rap1 activity, followed by its decrease. It is likely that RAPGEF2 accounts for the initial rise in Rap1 activity, although the role of other GEFs, such as C3G, cannot be ruled out at this stage. It has been shown that RAPGEF2 acts not only as an upstream activator of Rap1, but is in turn activated by Rap1-GTP, via direct association of its RA domain with Rap1-GTP (Hisata et al., 2007; Liao et al., 1999, 2001). This ensures that once activated, RAPGEF2 triggers a positive activation loop leading to the amplification of Rap1-mediated signaling. We propose that IKKβ- and CK1α-mediated degradation of RAPGEF2 represents a mechanism to stop the RAPGEF2-Rap1-GTP auto-amplification loop and inactivate Rap1-mediated signaling, enabling cell migration.

The direct involvement of IKKβ in the degradation of RAPGEF2 is intriguing. Indeed, the IKK complex is the major signaling node of the NF-κB pathway, which regulates immune and inflammatory responses. It is well established that inflammatory cells, and in particular, tumor-associated macrophages, are present at the invasive front of carcinomas where they stimulate motility of tumor cells. Tumor-associated macrophages secrete proinflammatory cytokines, such as TNFα, which activate the IKK complex and the downstream NF-κB signaling. By inducing RAPGEF2 degradation and consequent inhibition of Rap, a potent and ubiquitous activator of integrins, IKK would directly control integrin-mediated epithelial cell adhesion, migration, and polarity.

Although a number of molecular mechanisms underlying the prometastatic function of the NF-κB signaling pathway have been proposed, these are all based on the ability of NF-κB transcription factors to translocate into the nucleus and control the expression of genes involved in EMT (Snail), invasion, (matrix metalloproteinase-9), and survival (BCL-XL, XIAP). Our study suggests that the IKK complex can mediate motility and invasiveness of cancer cells in both transcription-dependent (via the activation of NF-κB transcription factors) and -independent (via degradation of the Rap1 activator RAPGEF2) manners.

Of note, we observe proteasome-dependent degradation of RAPGEF2 in response to phorbol esters or HGF, regarded as weaker activators of IKK if compared with proinflammatory cytokines such as TNFα (Fan et al., 2005, 2007, 2009; Hah and Lee, 2003; Huang et al., 2003; Müller et al., 2002). Interestingly, we detect an accelerated degradation of RAPGEF2 when cells are treated with both HGF and TNFα, suggesting a synergistic action of these two growth factors on RAPGEF2 proteolysis (Figure S4R).

In conclusion, we have shown that HGF induces rapid proteasomal degradation of the Rap activator RAPGEF2 and that expression of a nondegradable mutant of RAPGEF2 inhibits epithelial cell migration. Moreover, we have demonstrated that inhibition of RAPGEF2 degradation dramatically suppresses invasion and dissemination of breast cancer cells. A plethora of genetic and biochemical data have demonstrated that HGF, produced by stromal cells, and its tyrosine kinase receptor MET, present in tumor cells, play a causal role in metastasis formation during cancer progression. Notably, somatic and germline mutations, as well as amplification of the MET locus, are frequently found in human tumors. We suggest that, by inhibiting epithelial cell motility and invasion, degradation-resistant forms of RAPGEF2 might provide beneficial effects against the metastatic spread of cancer cells.

EXPERIMENTAL PROCEDURES

Gene Silencing by Small Interfering RNA

The sequence and validation of the oligonucleotides corresponding to βTrCP1 and βTrCP2 were previously published (Guardavaccaro et al., 2008). Cells were transfected with the oligonucleotides twice (24 and 48 hr after plating) using Oligofectamine (Invitrogen) according to manufacturer's recommendations. Forty-eight hours after the last transfection, lysates were prepared and analyzed by immunoblotting.

Zebrafish

All zebrafish strains were maintained at the Hubrecht Institute under standard husbandry conditions. The transgenic line used was *Tg(fli1a:egfp)*^{y1} (Lawson and Weinstein, 2002).

Invasion Assay in Zebrafish

Zebrafish were grown in 75 μM 1-phenyl 2-thiourea (PTU) (Sigma-Aldrich) dissolved in E3 medium (5 mM NaCl, 0.17 mM KCl, 0.33 mM $CaCl_2$, 0.33 mM $MgSO_4$). Cells for injections were labeled with the lipophilic tracer DiI (Invitrogen) 12 hr before injection. Cells were trypsinized and dissolved in PBS at the concentration of 400 cells/nl. Approximately 800 cells (2 nl) were injected into the perivitelline space of 48 hpf zebrafish embryos. Neovascularization and metastasis were monitored and quantified.

Imaging of Zebrafish Embryos

Embryos were mounted in 0.5%–1% low melting point agarose (Invitrogen) dissolved in E3 medium (5 mM NaCl, 0.17 mM KCl, 0.33 mM $CaCl_2$, 0.33 mM $MgSO_4$) on a culture dish with a glass coverslip replacing the bottom. Imaging was performed with a Leica SP2 confocal microscope (Leica Microsystems) using a 10× or 20× objective with digital zoom.

SUPPLEMENTAL INFORMATION

Supplemental Information includes Supplemental Experimental Procedures and four figures and can be found with this article online at http://dx.doi.org/10.1016/j.devcel.2013.10.023.

ACKNOWLEDGMENTS

We thank R. Bolder, R. Lim, and the Hubrecht Imaging Center (HIC) for their contributions, A. Ciechanover, M. Karin, I. Larik, J. Beaudouin, J. den Hertog, N. Geijsen, H. Clevers, F. Galvagni, and W. Wei for reagents, and S. Schulte-Merker for helpful comments and discussion. Work in D.G.'s laboratory was supported by the Royal Dutch Academy of Arts and Sciences (KNAW), the Dutch Cancer Society (KWF), the Cancer Genomics Centre, and the European Union under Marie Curie Actions (FP7). A.d.B. was supported by Netherlands Organization for Scientific Research (NWO). T.Y.L., S.M., and A.J.R.H. were supported by the Netherlands Proteomics Center (NPC).

Received: June 25, 2013
Revised: October 4, 2013
Accepted: October 29, 2013
Published: November 27, 2013

REFERENCES

Ahmed, S.M., Thériault, B.L., Uppalapati, M., Chiu, C.W., Gallie, B.L., Sidhu, S.S., and Angers, S. (2012). KIF14 negatively regulates Rap1a-Radil signaling during breast cancer progression. J. Cell Biol. *199*, 951–967.

Arai, A., Nosaka, Y., Kanda, E., Yamamoto, K., Miyasaka, N., and Miura, O. (2001). Rap1 is activated by erythropoietin or interleukin-3 and is involved in regulation of beta1 integrin-mediated hematopoietic cell adhesion. J. Biol. Chem. *276*, 10453–10462.

Bilasy, S.E., Satoh, T., Ueda, S., Wei, P., Kanemura, H., Aiba, A., Terashima, T., and Kataoka, T. (2009). Dorsal telencephalon-specific RA-GEF-1 knockout mice develop heterotopic cortical mass and commissural fiber defect. Eur. J. Neurosci. *29*, 1994–2008.

Boettner, B., and Van Aelst, L. (2009). Control of cell adhesion dynamics by Rap1 signaling. Curr. Opin. Cell Biol. *21*, 684–693.

Bos, J.L. (2005). Linking Rap to cell adhesion. Curr. Opin. Cell Biol. *17*, 123–128.

Bos, J.L., de Rooij, J., and Reedquist, K.A. (2001). Rap1 signalling: adhering to new models. Nat. Rev. Mol. Cell Biol. *2*, 369–377.

Cardozo, T., and Pagano, M. (2004). The SCF ubiquitin ligase: insights into a molecular machine. Nat. Rev. Mol. Cell Biol. *5*, 739–751.

Caron, E., Self, A.J., and Hall, A. (2000). The GTPase Rap1 controls functional activation of macrophage integrin alphaMbeta2 by LPS and other inflammatory mediators. Curr. Biol. *10*, 974–978.

de Rooij, J., Boenink, N.M., van Triest, M., Cool, R.H., Wittinghofer, A., and Bos, J.L. (1999). PDZ-GEF1, a guanine nucleotide exchange factor specific for Rap1 and Rap2. J. Biol. Chem. *274*, 38125–38130.

de Rooij, J., Kerstens, A., Danuser, G., Schwartz, M.A., and Waterman-Storer, C.M. (2005). Integrin-dependent actomyosin contraction regulates epithelial cell scattering. J. Cell Biol. *171*, 153–164.

Duchniewicz, M., Zemojtel, T., Kolanczyk, M., Grossmann, S., Scheele, J.S., and Zwartkruis, F.J. (2006). Rap1A-deficient T and B cells show impaired integrin-mediated cell adhesion. Mol. Cell. Biol. *26*, 643–653.

Fan, S., Gao, M., Meng, Q., Laterra, J.J., Symons, M.H., Coniglio, S., Pestell, R.G., Goldberg, I.D., and Rosen, E.M. (2005). Role of NF-kappaB signaling in hepatocyte growth factor/scatter factor-mediated cell protection. Oncogene *24*, 1749–1766.

Fan, S., Meng, Q., Laterra, J.J., and Rosen, E.M. (2007). Ras effector pathways modulate scatter factor-stimulated NF-kappaB signaling and protection against DNA damage. Oncogene *26*, 4774–4796.

Fan, S., Meng, Q., Laterra, J.J., and Rosen, E.M. (2009). Role of Src signal transduction pathways in scatter factor-mediated cellular protection. J. Biol. Chem. *284*, 7561–7577.

Freeman, S.A., McLeod, S.J., Dukowski, J., Austin, P., Lee, C.C., Millen-Martin, B., Kubes, P., McCafferty, D.M., Gold, M.R., and Roskelley, C.D. (2010). Preventing the activation or cycling of the Rap1 GTPase alters adhesion and cytoskeletal dynamics and blocks metastatic melanoma cell extravasation into the lungs. Cancer Res. *70*, 4590–4601.

Frescas, D., and Pagano, M. (2008). Deregulated proteolysis by the F-box proteins SKP2 and beta-TrCP: tipping the scales of cancer. Nat. Rev. Cancer *8*, 438–449.

Gao, D., Inuzuka, H., Tan, M.K., Fukushima, H., Locasale, J.W., Liu, P., Wan, L., Zhai, B., Chin, Y.R., Shaik, S., et al. (2011). mTOR drives its own activation via SCF(βTrCP)-dependent degradation of the mTOR inhibitor DEPTOR. Mol. Cell *44*, 290–303.

Gherardi, E., Gray, J., Stoker, M., Perryman, M., and Furlong, R. (1989). Purification of scatter factor, a fibroblast-derived basic protein that modulates epithelial interactions and movement. Proc. Natl. Acad. Sci. USA *86*, 5844–5848.

Guardavaccaro, D., Frescas, D., Dorrello, N.V., Peschiaroli, A., Multani, A.S., Cardozo, T., Lasorella, A., Iavarone, A., Chang, S., Hernando, E., and Pagano, M. (2008). Control of chromosome stability by the beta-TrCP-REST-Mad2 axis. Nature *452*, 365–369.

Hah, N., and Lee, S.T. (2003). An absolute role of the PKC-dependent NF-kappaB activation for induction of MMP-9 in hepatocellular carcinoma cells. Biochem. Biophys. Res. Commun. *305*, 428–433.

Hisata, S., Sakisaka, T., Baba, T., Yamada, T., Aoki, K., Matsuda, M., and Takai, Y. (2007). Rap1-PDZ-GEF1 interacts with a neurotrophin receptor at late endosomes, leading to sustained activation of Rap1 and ERK and neurite outgrowth. J. Cell Biol. *178*, 843–860.

Hogan, C., Serpente, N., Cogram, P., Hosking, C.R., Bialucha, C.U., Feller, S.M., Braga, V.M., Birchmeier, W., and Fujita, Y. (2004). Rap1 regulates the formation of E-cadherin-based cell-cell contacts. Mol. Cell. Biol. *24*, 6690–6700.

Huang, W.C., Chen, J.J., Inoue, H., and Chen, C.C. (2003). Tyrosine phosphorylation of I-kappa B kinase alpha/beta by protein kinase C-dependent c-Src activation is involved in TNF-alpha-induced cyclooxygenase-2 expression. J. Immunol. *170*, 4767–4775.

Jin, J., Cardozo, T., Lovering, R.C., Elledge, S.J., Pagano, M., and Harper, J.W. (2004). Systematic analysis and nomenclature of mammalian F-box proteins. Genes Dev. *18*, 2573–2580.

Katagiri, K., Hattori, M., Minato, N., Irie, Sk., Takatsu, K., and Kinashi, T. (2000). Rap1 is a potent activation signal for leukocyte function-associated antigen 1 distinct from protein kinase C and phosphatidylinositol-3-OH kinase. Mol. Cell. Biol. *20*, 1956–1969.

Katagiri, K., Maeda, A., Shimonaka, M., and Kinashi, T. (2003). RAPL, a Rap1-binding molecule that mediates Rap1-induced adhesion through spatial regulation of LFA-1. Nat. Immunol. *4*, 741–748.

Kim, W.J., Gersey, Z., and Daaka, Y. (2012). Rap1GAP regulates renal cell carcinoma invasion. Cancer Lett. *320*, 65–71.

Kinbara, K., Goldfinger, L.E., Hansen, M., Chou, F.L., and Ginsberg, M.H. (2003). Ras GTPases: integrins' friends or foes? Nat. Rev. Mol. Cell Biol. *4*, 767–776.

Kitayama, H., Sugimoto, Y., Matsuzaki, T., Ikawa, Y., and Noda, M. (1989). A ras-related gene with transformation suppressor activity. Cell *56*, 77–84.

Knox, A.L., and Brown, N.H. (2002). Rap1 GTPase regulation of adherens junction positioning and cell adhesion. Science *295*, 1285–1288.

Kooistra, M.R., Dubé, N., and Bos, J.L. (2007). Rap1: a key regulator in cell-cell junction formation. J. Cell Sci. *120*, 17–22.

Kruiswijk, F., Yuniati, L., Magliozzi, R., Low, T.Y., Lim, R., Bolder, R., Mohammed, S., Proud, C.G., Heck, A.J., Pagano, M., and Guardavaccaro, D. (2012). Coupled activation and degradation of eEF2K regulates protein synthesis in response to genotoxic stress. Sci. Signal. *5*, ra40.

Kuiperij, H.B., de Rooij, J., Rehmann, H., van Triest, M., Wittinghofer, A., Bos, J.L., and Zwartkruis, F.J. (2003). Characterisation of PDZ-GEFs, a family of guanine nucleotide exchange factors specific for Rap1 and Rap2. Biochim. Biophys. Acta *1593*, 141–149.

Lawson, N.D., and Weinstein, B.M. (2002). In vivo imaging of embryonic vascular development using transgenic zebrafish. Dev. Biol. *248*, 307–318.

Lee, J.H., Cho, K.S., Lee, J., Kim, D., Lee, S.B., Yoo, J., Cha, G.H., and Chung, J. (2002). Drosophila PDZ-GEF, a guanine nucleotide exchange factor for Rap1 GTPase, reveals a novel upstream regulatory mechanism in the mitogen-activated protein kinase signaling pathway. Mol. Cell. Biol. *22*, 7658–7666.

Lee, S.L., Rouhi, P., Dahl Jensen, L., Zhang, D., Ji, H., Hauptmann, G., Ingham, P., and Cao, Y. (2009). Hypoxia-induced pathological angiogenesis mediates tumor cell dissemination, invasion, and metastasis in a zebrafish tumor model. Proc. Natl. Acad. Sci. USA *106*, 19485–19490.

Liao, Y., Kariya, K., Hu, C.D., Shibatohge, M., Goshima, M., Okada, T., Watari, Y., Gao, X., Jin, T.G., Yamawaki-Kataoka, Y., and Kataoka, T. (1999). RA-GEF, a novel Rap1A guanine nucleotide exchange factor containing a Ras/Rap1A-associating domain, is conserved between nematode and humans. J. Biol. Chem. *274*, 37815–37820.

Liao, Y., Satoh, T., Gao, X., Jin, T.G., Hu, C.D., and Kataoka, T. (2001). RA-GEF-1, a guanine nucleotide exchange factor for Rap1, is activated by translocation induced by association with Rap1*GTP and enhances Rap1-dependent B-Raf activation. J. Biol. Chem. *276*, 28478–28483.

Loerke, D., le Duc, Q., Blonk, I., Kerstens, A., Spanjaard, E., Machacek, M., Danuser, G., and de Rooij, J. (2012). Quantitative imaging of epithelial cell scattering identifies specific inhibitors of cell motility and cell-cell dissociation. Sci. Signal. *5*, rs5.

Low, T.Y., Magliozzi, R., Guardavaccaro, D., and Heck, A.J. (2013). Unraveling the ubiquitin-regulated signaling networks by mass spectrometry-based proteomics. Proteomics *13*, 526–537.

Lyle, K.S., Raaijmakers, J.H., Bruinsma, W., Bos, J.L., and de Rooij, J. (2008). cAMP-induced Epac-Rap activation inhibits epithelial cell migration by modulating focal adhesion and leading edge dynamics. Cell. Signal. *20*, 1104–1116.

McSherry, E.A., Brennan, K., Hudson, L., Hill, A.D., and Hopkins, A.M. (2011). Breast cancer cell migration is regulated through junctional adhesion molecule-A-mediated activation of Rap1 GTPase. Breast Cancer Res. *13*, R31.

Müller, M., Morotti, A., and Ponzetto, C. (2002). Activation of NF-kappaB is essential for hepatocyte growth factor-mediated proliferation and tubulogenesis. Mol. Cell. Biol. *22*, 1060–1072.

Ohba, Y., Ikuta, K., Ogura, A., Matsuda, J., Mochizuki, N., Nagashima, K., Kurokawa, K., Mayer, B.J., Maki, K., Miyazaki, J., and Matsuda, M. (2001). Requirement for C3G-dependent Rap1 activation for cell adhesion and embryogenesis. EMBO J. *20*, 3333–3341.

Ohtsuka, T., Hata, Y., Ide, N., Yasuda, T., Inoue, E., Inoue, T., Mizoguchi, A., and Takai, Y. (1999). nRap GEP: a novel neural GDP/GTP exchange protein for rap1 small G protein that interacts with synaptic scaffolding molecule (S-SCAM). Biochem. Biophys. Res. Commun. *265*, 38–44.

Pannekoek, W.J., Kooistra, M.R., Zwartkruis, F.J., and Bos, J.L. (2009). Cell-cell junction formation: the role of Rap1 and Rap1 guanine nucleotide exchange factors. Biochim. Biophys. Acta *1788*, 790–796.

Pellis-van Berkel, W., Verheijen, M.H., Cuppen, E., Asahina, M., de Rooij, J., Jansen, G., Plasterk, R.H., Bos, J.L., and Zwartkruis, F.J. (2005). Requirement of the Caenorhabditis elegans RapGEF pxf-1 and rap-1 for epithelial integrity. Mol. Biol. Cell *16*, 106–116.

Price, L.S., Hajdo-Milasinovic, A., Zhao, J., Zwartkruis, F.J., Collard, J.G., and Bos, J.L. (2004). Rap1 regulates E-cadherin-mediated cell-cell adhesion. J. Biol. Chem. *279*, 35127–35132.

Rebhun, J.F., Castro, A.F., and Quilliam, L.A. (2000). Identification of guanine nucleotide exchange factors (GEFs) for the Rap1 GTPase. Regulation of MR-GEF by M-Ras-GTP interaction. J. Biol. Chem. *275*, 34901–34908.

Reedquist, K.A., Ross, E., Koop, E.A., Wolthuis, R.M., Zwartkruis, F.J., van Kooyk, Y., Salmon, M., Buckley, C.D., and Bos, J.L. (2000). The small GTPase, Rap1, mediates CD31-induced integrin adhesion. J. Cell Biol. *148*, 1151–1158.

Rosen, E.M., Goldberg, I.D., Liu, D., Setter, E., Donovan, M.A., Bhargava, M., Reiss, M., and Kacinski, B.M. (1991). Tumor necrosis factor stimulates epithelial tumor cell motility. Cancer Res. *51*, 5315–5321.

Sakkab, D., Lewitzky, M., Posern, G., Schaeper, U., Sachs, M., Birchmeier, W., and Feller, S.M. (2000). Signaling of hepatocyte growth factor/scatter factor (HGF) to the small GTPase Rap1 via the large docking protein Gab1 and the adapter protein CRKL. J. Biol. Chem. *275*, 10772–10778.

Satyanarayana, A., Gudmundsson, K.O., Chen, X., Coppola, V., Tessarollo, L., Keller, J.R., and Hou, S.X. (2010). RapGEF2 is essential for embryonic hematopoiesis but dispensable for adult hematopoiesis. Blood *116*, 2921–2931.

Sebzda, E., Bracke, M., Tugal, T., Hogg, N., and Cantrell, D.A. (2002). Rap1A positively regulates T cells via integrin activation rather than inhibiting lymphocyte signaling. Nat. Immunol. *3*, 251–258.

Spahn, P., Ott, A., and Reuter, R. (2012). The PDZ-GEF protein Dizzy regulates the establishment of adherens junctions required for ventral furrow formation in Drosophila. J. Cell Sci. *125*, 3801–3812.

Stoker, M., and Perryman, M. (1985). An epithelial scatter factor released by embryo fibroblasts. J. Cell Sci. *77*, 209–223.

Stoker, M., Gherardi, E., Perryman, M., and Gray, J. (1987). Scatter factor is a fibroblast-derived modulator of epithelial cell mobility. Nature *327*, 239–242.

Tanimura, S., Chatani, Y., Hoshino, R., Sato, M., Watanabe, S., Kataoka, T., Nakamura, T., and Kohno, M. (1998). Activation of the 41/43 kDa mitogen-activated protein kinase signaling pathway is required for hepatocyte growth factor-induced cell scattering. Oncogene *17*, 57–65.

Tapia, J.C., Torres, V.A., Rodriguez, D.A., Leyton, L., and Quest, A.F. (2006). Casein kinase 2 (CK2) increases survivin expression via enhanced beta-catenin-T cell factor/lymphoid enhancer binding factor-dependent transcription. Proc. Natl. Acad. Sci. USA *103*, 15079–15084.

Thiery, J.P. (2002). Epithelial-mesenchymal transitions in tumour progression. Nat. Rev. Cancer *2*, 442–454.

Wang, H., Singh, S.R., Zheng, Z., Oh, S.W., Chen, X., Edwards, K., and Hou, S.X. (2006). Rap-GEF signaling controls stem cell anchoring to their niche through regulating DE-cadherin-mediated cell adhesion in the Drosophila testis. Dev. Cell *10*, 117–126.

Wei, P., Satoh, T., Edamatsu, H., Aiba, A., Setsu, T., Terashima, T., Kitazawa, S., Nakao, K., Yoshikawa, Y., Tamada, M., and Kataoka, T. (2007). Defective vascular morphogenesis and mid-gestation embryonic death in mice lacking RA-GEF-1. Biochem. Biophys. Res. Commun. *363*, 106–112.

Wu, G., Xu, G., Schulman, B.A., Jeffrey, P.D., Harper, J.W., and Pavletich, N.P. (2003). Structure of a beta-TrCP1-Skp1-beta-catenin complex: destruction motif binding and lysine specificity of the SCF(beta-TrCP1) ubiquitin ligase. Mol. Cell *11*, 1445–1456.

Yajnik, V., Paulding, C., Sordella, R., McClatchey, A.I., Saito, M., Wahrer, D.C., Reynolds, P., Bell, D.W., Lake, R., van den Heuvel, S., et al. (2003). DOCK4, a GTPase activator, is disrupted during tumorigenesis. Cell *112*, 673–684.

Yang, J., and Weinberg, R.A. (2008). Epithelial-mesenchymal transition: at the crossroads of development and tumor metastasis. Dev. Cell *14*, 818–829.

Zhang, L., Zhou, F., Drabsch, Y., Gao, R., Snaar-Jagalska, B.E., Mickanin, C., Huang, H., Sheppard, K.A., Porter, J.A., Lu, C.X., and ten Dijke, P. (2012). USP4 is regulated by AKT phosphorylation and directly deubiquitylates TGF-β type I receptor. Nat. Cell Biol. *14*, 717–726.

Zheng, H., Gao, L., Feng, Y., Yuan, L., Zhao, H., and Cornelius, L.A. (2009). Down-regulation of Rap1GAP via promoter hypermethylation promotes melanoma cell proliferation, survival, and migration. Cancer Res. *69*, 449–457.

Developmental Cell, Volume *27*

Supplemental Information

Control of Epithelial Cell Migration and Invasion by the IKKβ- and CK1α-Mediated Degradation of RAPGEF2

Roberto Magliozzi, Teck Yew Low, Bart G.M.W. Weijts, Tianhong Cheng, Emma Spanjaard, Shabaz Mohammed, Anouk van Veen, Huib Ovaa, Johan de Rooij, Fried J.T. Zwartkruis, Johannes L. Bos, Alain de Bruin, Albert J.R. Heck, and Daniele Guardavaccaro

Inventory of Supplemental Information

SUPPLEMENTAL FIGURES AND LEGENDS

Figure S1. Continued on the next page.

Figure S1 (continued). βTrCP targets RAPGEF2 for degradation in response to HGF, Related to Figure 1

(A) Peptide coverage of RAPGEF2 in the mass spectrometry analysis of βTrCP2 immunopurification.

(B) Peptide coverage of βTrCP1/FBXW1, βTrCP2/FBXW11, Cul1, Skp1 and Rbx1 in the mass spectrometry analysis of RAPGEF2 immunopurification.

(C) Peptide coverage of Rap1A, Rap1B, Rap2B and Rap2C in the mass spectrometry analysis of RAPGEF2 immunopurification.

Amino acid sequences of detected unique peptides are highlighted in yellow.

(D, E) MDCK cells were treated with EGF (D) or IGF (E), collected at the indicated times and lysed. Whole cell extracts were analyzed by immunoblotting. Cul1 is shown as a loading control.

(F) HEK293 cells were treated with HGF in the presence or absence of the proteasome inhibitor MG132. Cells were collected at the indicated times and lysed. Whole cell extracts were subjected to immunoblotting. Actin is shown as a loading control.

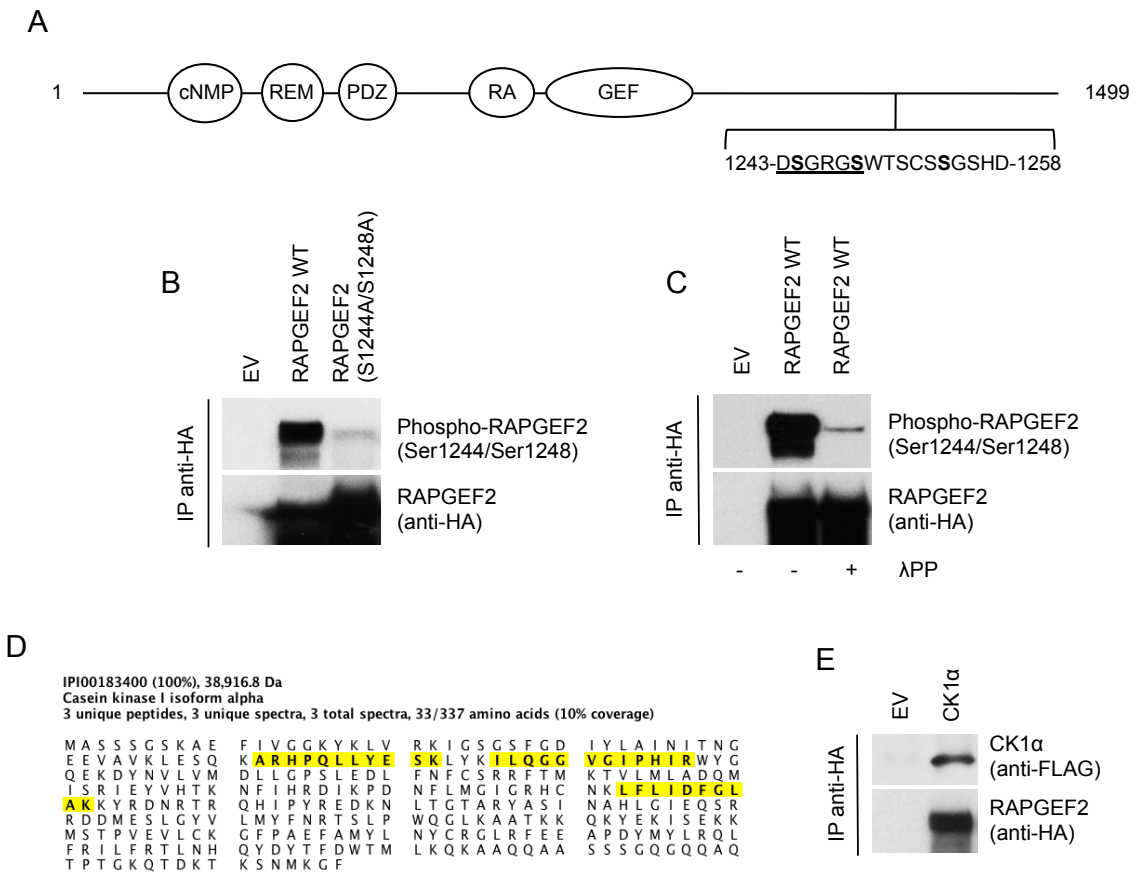

Figure S2. The RAPGEF2 degron is phosphorylated by CK1α, Related to Figure 2
(A) Graphical summary of the RAPGEF2 conserved domains. Sequence and position of the βTrCP-binding domain are shown.
(B) HEK293 cells expressing either HA-tagged wild type RAPGEF2 or HA-tagged RAPGEF2(S1244A/S1248A) were treated with HGF and MG132 for 4 hours before harvesting. Whole cell extracts were immunoprecipitated with anti-HA resin followed by immunoblotting with antibodies specific for the indicated proteins.
(C) HEK293 cells expressing HA-tagged wild type RAPGEF2 were treated with HGF and MG132 for 4 hours before harvesting. Whole cell extracts were subjected to immunoprecipitation with anti-HA resin. When indicated, the immunocomplexes were incubated with lambda phosphatase for 30 minutes and then subjected to immunoblotting with antibodies specific for the indicated proteins.
(D) Peptide coverage of CK1α in the mass spectrometry analysis of RAPGEF2 immunopurification. Amino acid sequences of detected unique peptides are highlighted in yellow.
(E) HEK293T cells were transfected with the indicated plasmids. After 48 hours, cells were treated with MG132 for 5 hours. Cells were lysed and whole cell extracts were subjected to immunoprecipitation using anti-HA resin before immunoblotting with antibodies for the indicated proteins.

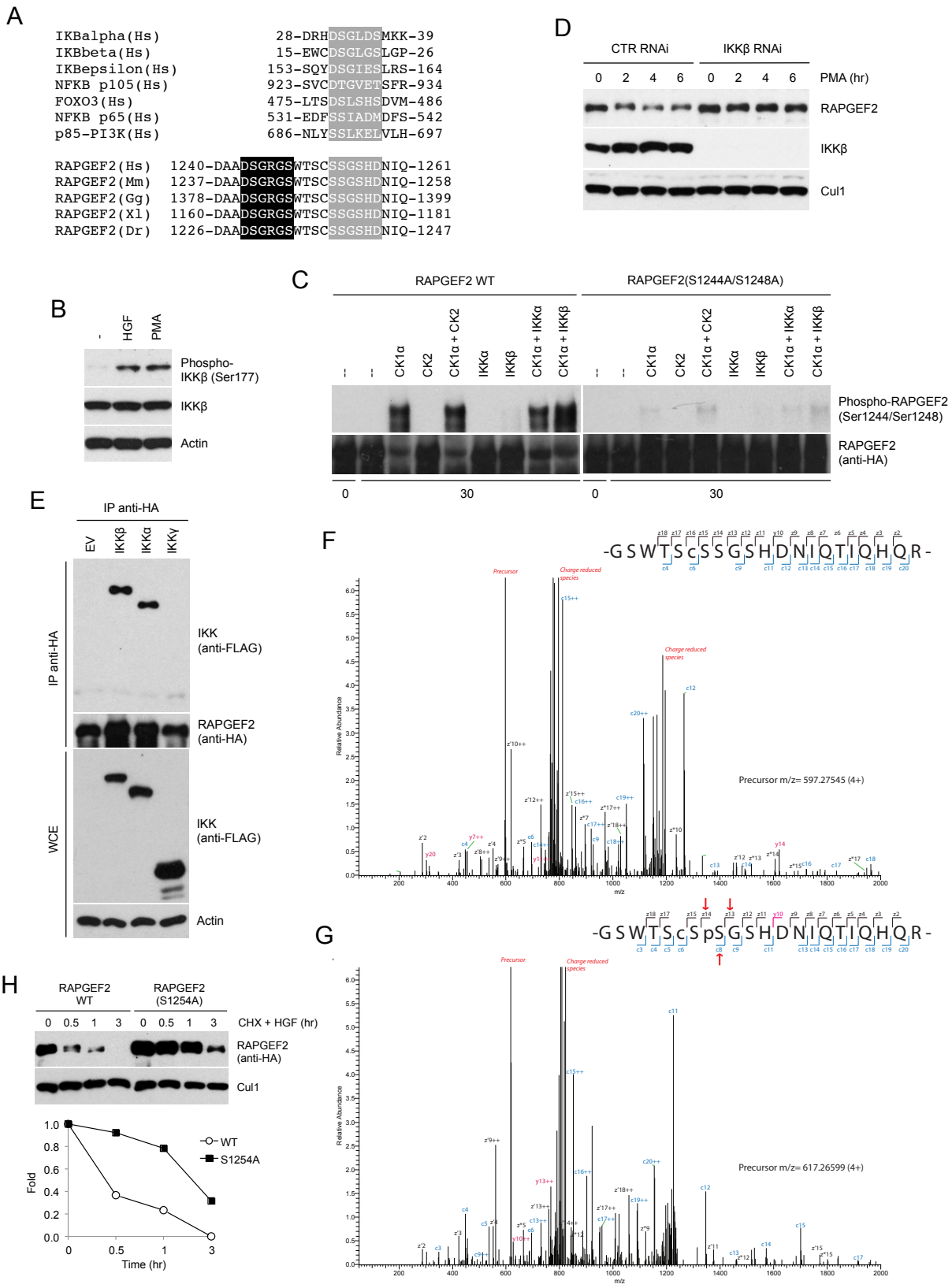

Figure S3. Continued on the next page.

Figure S3 (continued). IKKβ-mediated phosphorylation of RAPGEF2, Related to Figure 3

(A) Alignment of the amino acid regions corresponding to IKK target sites in RAPGEF2 orthologs and previously reported IKK substrates (highlighted in grey). The upstream RAPGEF2 degron is highlighted in black.

(B) Cells were treated as indicated, collected and lysed. Whole cell extracts were subjected to immunoblotting with antibodies specific for the indicated proteins.

(C) Immunopurified wild type RAPGEF2 or RAPGEF2(S1244A/S1248A) were first dephosphorylated by treatment with lambda phosphatase and then incubated with the indicated purified kinases in the presence of ATP. Reactions were stopped by adding Laemmli buffer and analyzed by immunoblotting with antibodies for the indicated proteins.

(D) Cells were transfected with the indicated siRNA oligonucleotides and treated with PMA. Cells were then collected at the indicated times and lysed. Whole cell extracts were analyzed by immunoblotting with antibodies specific for the indicated proteins. Cul1 is shown as a loading control

(E) HEK293T cells were transfected with the indicated cDNAs. After 48 hours, cells were treated with MG132 for 5 hours. Cells were lysed and whole cell extracts were subjected to immunoprecipitation using anti-HA resin before immunoblotting with antibodies for the indicated proteins.

(F, G) RAPGEF2 was immunopurified and dephosphorylated with lambda phosphatase prior to an *in vitro* kinase assay in the presence of purified IKKβ, CK1α, CK2, or RSK1. A mock reaction (no kinase) was used as a negative control. Individual mixes were subsequently trypsinized and analyzed by mass spectrometry. The RAPGEF2 tryptic peptide GSWTSCSSGSHDNIQTIQHQR was not found to be phosphorylated in any mix (F) except when IKKβ was used in the *in vitro* kinase assay. In this sample, the same peptide was found to be phosphorylated on Ser1254 (G). As shown, both peptide sequences can be explained by their respective ETD MSMS spectrum (Mascot Score 48 and 52), including the pS1254 site (PhosphoRS site probability = 94.4%). In this figure, [c] denotes carbaminomethylated cysteine; [pS] denotes phosphorylated serine; [z'] denotes z+1 ions and [z*] denotes z+2 ions.

(H) MDCK cells, transduced with lentiviruses expressing HA-tagged wild type RAPGEF2 or HA-tagged RAPGEF2(S1254A), were treated with HGF and the inhibitor of protein synthesis cycloheximide (CHX). Cells were then collected and analyzed by immunoblotting with antibodies for the indicated proteins. Cul1 is shown as a loading control. The graph illustrates the quantification of RAPGEF2 abundance relative to the amount at time 0.

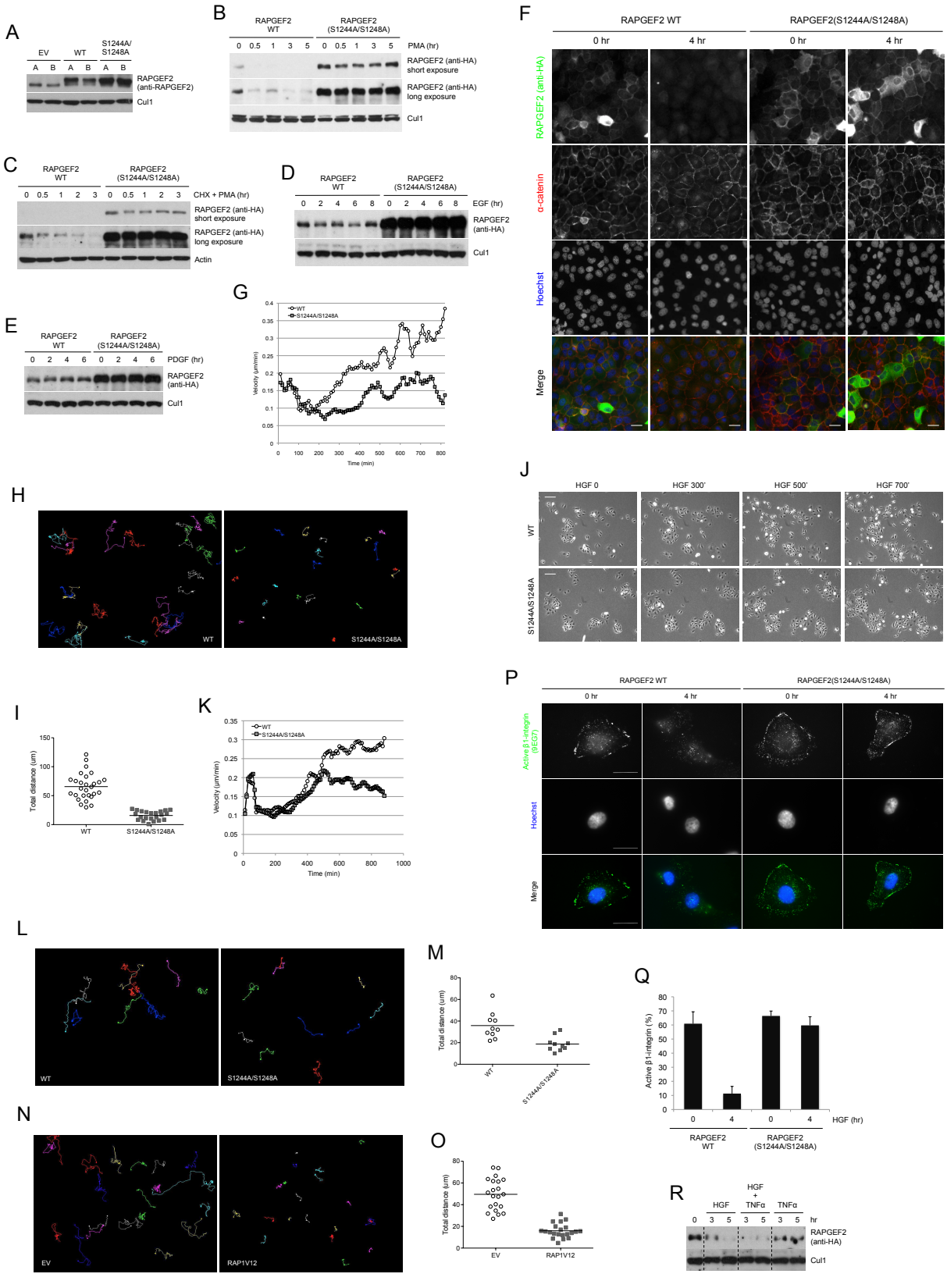

Figure S4. Continued on the next page.

Figure S4 (continued). RAPGEF2 degradation is required for induction of cell migration in response to HGF. Related to Figure 4

(A) Cells were mock-transduced or transduced with lentiviruses expressing HA-tagged wild type RAPGEF2 or RAPGEF2(S1244A/S1248A). Cells were collected and lysed. Whole cell extracts were analyzed by immunoblotting. A and B indicate cells from independent lentiviral transductions.

(B) HEK293 cells transduced with lentiviruses expressing HA-tagged wild type RAPGEF2 or RAPGEF2(S1244A/S1248A) were treated with PMA. Cells were collected and analyzed by immunoblotting. Cul1 is shown as a loading control.

(C) HEK293 cells, transduced as in (B), were treated with PMA and the inhibitor of protein synthesis cycloheximide (CHX). Cells were then collected and analyzed by immunoblotting. Actin is shown as a loading control.

(D, E) MDCK cells, transduced as in (A), were treated with EGF (D) or PDGF (E). Cells were then collected and analyzed by immunoblotting. Cul1 is shown as a loading control.

(F) MDCK cells, transduced as in (A), were treated with HGF for 4 hours. Cells were analyzed by indirect immunofluorescence. Scale bars, 50 μm.

(G) An automated cell tracking software was employed to measure the average migration velocity of MDCK cells expressing wild type RAPGEF2 or RAPGEF2(S1244A/S1248A) in response to HGF. Only non-contacted cells (not starting from cell islands) were tracked. For each cell line/condition, 3 independent time-lapse image series (at least 300 individual cells) were analyzed.

(H) Representative individual migratory tracks of non-contacted MDCK cells expressing wild type RAPGEF2 or RAPGEF2(S1244A/S1248A) in response to HGF.

(I) Track distance of individual cells shown in (H). $P < 0.001$ (Student's t-test).

(J) MDCK cells transduced with lentiviruses expressing wild type RAPGEF2 or RAPGEF2(S1244A/S1248A) were cultured in low calcium (20 μM Ca^{2+}). Cells were treated with HGF and imaged by time-lapse phase-contrast microscopy. Representative phase-contrast images from the time-lapse series are shown. Scale bars, 100 μm.

(K) An automated cell tracking software was employed to measure the average migration velocity of MDCK cells expressing wild type RAPGEF2 or RAPGEF2(S1244A/S1248A) cultured in 20 μM Ca^{2+} in the presence of HGF. For each cell line/condition, 3 independent time-lapse image series were analyzed.

(L) Representative individual migratory tracks of MDCK cells expressing wild type RAPGEF2 or RAPGEF2(S1244A/S1248A) cultured in 20 μM Ca^{2+} with HGF.

(M) Track distance of individual cells shown in (L). Horizontal lines represent the mean. $P = 0.00134$ (Student's t-test).

(N) MDCK cells were transfected with either YFP or YFP-tagged Rap1V12 (a constitutively active Rap1 mutant). Cells were then treated with HGF and imaged by time-lapse microscopy for 12 hours. Representative individual migratory tracks of non-contacted cells are shown.

(O) Track distance of individual cells shown in (N). $P < 0.001$ (Student's t-test).

(P) MDCK cells transduced with lentiviruses expressing HA-tagged wild type RAPGEF2 or RAPGEF2(S1244A/S1248A) were treated with HGF for 4 hours or left untreated. Cells were analyzed by indirect immunofluorescence. Scale bars, 20 μm.

(Q) Quantification of immunofluorescence shown in (P). Cells were scored for bright edges ($n = 3$, ± SD). $P < 0.001$.

(R) MDCK cells were treated with the indicated growth factors. Whole cell extracts were subjected to immunoblotting. Cul1 is shown as a loading control. To facilitate comparison, dotted lines separate samples from cells treated with different growth factors.

EXTENDED EXPERIMENTAL PROCEDURES

Cell culture and drug treatment

HEK293T, HEK293, and MDCK cells were maintained in Dulbecco's modified Eagle's medium (Invitrogen) containing 10% fetal calf serum. To induce scattering, cells were serum starved for 16 hours and then treated with 10 ng/ml hepatocyte growth factor/scatter factor (HGF/SF, Sigma-Aldrich), or 10 ng/ml phorbol-12-myristate-13-acetate (PMA, Sigma-Aldrich). EGF, IGF and PDGF were used at 10 ng/ml. The following drugs were used: MG132 (Peptide Institute; 10 μM), TBB (Merck Millipore, 75 μM), D4476 (Sigma-Aldrich, 50 μM), IC261 (Sigma-Aldrich, 100 μM), SC-514 (Sigma-Aldrich, 20 μM), cycloheximide (Sigma-Aldrich, 100 μM).

Plasmids and small hairpin RNAs

The mammalian expression plasmid for CK1α was provided by H. Clevers. For lentivirus production, wild type RAPGEF2 and RAPGEF2(S1244A/S1248A) were subcloned into the lentiviral vector pHAGE2-EF1α. The RAPGEF2 mutant was generated using the QuickChange Site-directed Mutagenesis kit (Stratagene). shRNAs targeting human CK1α were provided by W. Wei. All cDNAs were sequenced.

Transient transfections and lentivirus-mediated gene transfer

HEK293 and HEK293T cells were transfected using the polyethylenimine (PEI) method. For lentivirus production, HEK293T cells were co-transfected with pHAGE2-EF1a and packaging vectors. Virus-containing medium was collected 48-72 hours after transfection and supplemented with 8 μg/ml polybrene. Cells were incubated with virus-containing medium for 6 hours for 2 consecutive days.

Purification of βTrCP2 interactors

HEK293T cells were transfected with pcDNA3-FLAG-HA-βTrCP2 and treated with 10 μM MG132 for 5 hours. Cells were harvested and subsequently lysed in lysis buffer (50 mM Tris-HCl pH 7.5, 150 mM NaCl, 1 mM EDTA, 0.5% NP40, plus protease and phosphatase inhibitors). βTrCP2 was immunopurified with anti-FLAG agarose resin (Sigma-Aldrich). After washing, proteins were eluted by competition with FLAG peptide (Sigma-Aldrich). The eluate was then subjected to a second immunopurification with anti-HA resin (12CA5 monoclonal antibody crosslinked to protein G Sepharose; Invitrogen) prior to elution in Laemmli sample buffer. The final eluate was separated by SDS-PAGE,

and proteins were visualized by Coomassie colloidal blue. Bands were sliced out from the gels and subjected to in-gel digestion. Gel pieces were then reduced, alkylated and digested according to a published protocol (Shevchenko et al., 1996). For mass spectrometric analysis, peptides recovered from in-gel digestion were separated with a C18 column and introduced by nano-electrospray into the LTQ Orbitrap XL (Thermo Fisher) with a configuration as described (Raijmakers et al., 2008). Peak lists were generated from the MS/MS spectra using MaxQuant build 1.0.13.13 (Cox and Mann, 2008), and then searched against the IPI Human database (version 3.37, 69164 entries) using Mascot search engine (Matrix Science). Carbaminomethylation (+57 Da) was set as fixed modification and protein N-terminal acetylation and methionine oxidation as variable modifications. Peptide tolerance was set to 7 ppm and fragment ion tolerance was set to 0.5 Da, allowing 2 missed cleavages with trypsin enzyme. Finally, Scaffold 3.6.1 (Proteome Software Inc.) was used to validate MS/MS based peptide and protein identifications. Peptide identifications were accepted if their Mascot scores exceeded 20.

Phosphorylation analysis by mass spectrometry

Samples were reduced with 10 mM DTT for 30 minutes at 60˚C, followed by addition of iodoacetamide to 20 mM followed by 30-minute incubation in the dark at room temperature. The first digestion was performed using Lys-C for 4 hours at 37˚C. Subsequently, the digest was diluted 5-fold using 50 mM ammonium bicarbonate to a final urea concentration of less than 2 M, and a second digestion with trypsin was performed overnight at 37˚C. Finally, the digestion was quenched by addition of formic acid to a final concentration of 0.1% (vol/vol). The resulting solution was desalted using 200 mg Sep-Pak C18 cartridges (Waters Corporation), lyophilized and reconstituted in 10% formic acid. LC-MS/MS was performed with both collision-induced dissociation and electron transfer dissociation in the form of data-dependent decision tree (Frese et al., 2011; Swaney et al., 2008). MS spectra to peptide sequence assignment is performed with Proteome Discoverer Version 1.3, with MASCOT version 2.3 as search engine and the localization of phosphorylated sites was evaluated with PhosphoRS version 2 (Taus et al., 2011).

Biochemical methods

Extract preparation, immunoprecipitation, and immunoblotting were previously described (Kruiswijk et al., 2012). Monoclonal antibodies were from Invitrogen (Cul1), Sigma-

Aldrich (FLAG), Santa Cruz Biotechnology (Actin), BD Biosciences (β-catenin, Rap2, active β1-integrin), Cell Signaling [IκBα, phospho-IκBα(Ser32/Ser36)] and Covance (HA). Rabbit polyclonal antibodies were from Cell Signaling [(βTrCP1, CK1α, IKKβ, phospho-IKKβ(Ser177)], Sigma-Aldrich (FLAG), Novus Biologicals (RAPGEF2) and Santa Cruz (Rap1).

***In vitro* kinase assay**

Immunopurified RAPGEF2 was first dephosphorylated by treatment with lambda phosphatase and then incubated at 30°C for 30 minutes with 0.2 mM ATP and the indicated kinases in a 20 μl of kinase buffer (25 mM Tris pH 7.5, 10 mM $MgCl_2$, 2 mM DTT, 5 mM β-glycerophosphate, 0.1 mM sodium orthovanadate). Reaction products were subjected to immunoblotting. Autoradiography was performed when γ^{32}P ATP was used. For sequential *in vitro* kinase assay (Figure 3B), immunopurified RAPGEF2 was subjected to a first phosphorylation reaction (30 minutes) with the indicated purified kinases. Samples were then washed three times in lysis buffer (50 mM Tris-HCl pH 7.5, 250 mM NaCl, 0.1% Triton X-100, 1 mM EGTA) to remove the first kinase and twice in kinase buffer. Samples were then subjected to a second phosphorylation reaction with CK1α as described above.

***In vitro* ubiquitylation assay**

RAPGEF2 ubiquitylation was performed in a volume of 10 µl containing $SCF^{\beta TrCP}$-RAPGEF2 immunocomplexes, 50 mM Tris pH 7.6, 5 mM $MgCl_2$, 0.6 mM DTT, 2 mM ATP, 1.5 ng/µl E1 (Boston Biochem), 10 ng/µl Ubc3, 2.5 µg/µl ubiquitin (Sigma-Aldrich), 1 µM ubiquitin aldehyde. The reactions were incubated at 30°C for 60 minutes and analyzed by immunoblotting.

Live cell microscopy

Cell scattering in MDCK cells was analyzed as previously described (Lyle et al., 2008). MDCK cells were seeded at low density in 48-well plates coated with 10 μg/ml collagen and allowed to grow in small colonies. The following day, cells were rinsed and incubated in Dulbecco's modified Eagle's medium containing 0.5 % FBS and 20 mM Hepes, pH 7.4. All wells were completely filled with medium and the plate was sealed using silicon grease and a glass plate. Images were acquired every 10 minutes using a 10X objective lens in a climate-controlled incubator. A robotic stage was used to

simultaneously collect images at different positions. Cells were imaged in absence of HGF for the first 2 hours, after which, 10 ng/ml HGF was added. Cells were then filmed for additional 12-16 hours. At least three time-lapse series were acquired for each condition in each experiment.

Analysis of cell scattering in time-lapse movies

The software employed to automatically track cell scattering has been previously described (Lyle et al., 2008). Briefly, this software detects and tracks single cells in the time-lapse images of scattering cells and determines their velocity throughout the process of scattering. Only cells that were faithfully tracked for at least 6 consecutive frames and stayed "single" during that period of time were considered. The velocity was calculated as the displacement (μm) over three consecutive frames, divided by the elapsed time (10 minutes).

Rap activation assay

Rap1 and Rap2 activity was analyzed as described (Franke et al., 1997).

Wound healing assay

Wound healing assay was performed as described (Buus et al., 2009). MDCK cells were seeded in a 6-well plate at 1 x 10^6 cells per well and starved overnight in 0.5% FBS containing medium. The following day, a linear scratch in the confluent cell monolayer was made with a sterile pipette tip. Cells were rinsed and supplemented with 10 ng/ml HGF for 8 hours. For each well 3 pictures were taken at 4X magnification along the scratch area.

Invasion assay in vitro

In vitro invasion assays were performed in 24-well ThinCert cell culture inserts (Greinerbioone, 8.0-μm pore size). MDA-MB-231 cells were serum starved overnight. The following day, 50 x 10^3 or 10 x 10^4 cells were plated in pre-coated transwell inserts (at least three replicas for each sample). HGF (10 ng/ml) was added to the lower compartment. After 8 hours, cells were fixed in 4% paraformaldehyde and stained with 0.5% crystal violet. Filters were photographed in 4 random fields and the number of cells counted. Every experiment was repeated independently at least three times.

Statistical analysis

Statistical analysis was performed using Pearson's Chi-Square or Student's t-test. Results with $P < 0.05$ were considered statistically significant.

Kruskal-Wallis and Dunn's post-hoc tests were used for the statistical analysis of the zebrafish xenograft experiments.

SUPPLEMENTAL REFERENCES

Buus, R., Faronato, M., Hammond, D.E., Urbe, S., and Clague, M.J. (2009). Deubiquitinase activities required for hepatocyte growth factor-induced scattering of epithelial cells. Curr Biol *19*, 1463-1466.

Cox, J., and Mann, M. (2008). MaxQuant enables high peptide identification rates, individualized p.p.b.-range mass accuracies and proteome-wide protein quantification. Nat Biotechnol *26*, 1367-1372.

Franke, B., Akkerman, J.W., and Bos, J.L. (1997). Rapid Ca2+-mediated activation of Rap1 in human platelets. The EMBO journal *16*, 252-259.

Frese, C.K., Altelaar, A.F., Hennrich, M.L., Nolting, D., Zeller, M., Griep-Raming, J., Heck, A.J., and Mohammed, S. (2011). Improved peptide identification by targeted fragmentation using CID, HCD and ETD on an LTQ-Orbitrap Velos. J Proteome Res *10*, 2377-2388.

Kruiswijk, F., Yuniati, L., Magliozzi, R., Low, T.Y., Lim, R., Bolder, R., Mohammed, S., Proud, C.G., Heck, A.J., Pagano, M.*, et al.* (2012). Coupled Activation and Degradation of eEF2K Regulates Protein Synthesis in Response to Genotoxic Stress. Science Signaling *5*, ra40.

Lyle, K.S., Raaijmakers, J.H., Bruinsma, W., Bos, J.L., and de Rooij, J. (2008). cAMP-induced Epac-Rap activation inhibits epithelial cell migration by modulating focal adhesion and leading edge dynamics. Cellular signalling *20*, 1104-1116.

Raijmakers, R., Berkers, C.R., de Jong, A., Ovaa, H., Heck, A.J., and Mohammed, S. (2008). Automated online sequential isotope labeling for protein quantitation applied to proteasome tissue-specific diversity. Mol Cell Proteomics *7*, 1755-1762.

Shevchenko, A., Wilm, M., Vorm, O., and Mann, M. (1996). Mass spectrometric sequencing of proteins silver-stained polyacrylamide gels. Anal Chem *68*, 850-858.

Swaney, D.L., McAlister, G.C., and Coon, J.J. (2008). Decision tree-driven tandem mass spectrometry for shotgun proteomics. Nat Methods *5*, 959-964.

Taus, T., Kocher, T., Pichler, P., Paschke, C., Schmidt, A., Henrich, C., and Mechtler, K. (2011). Universal and confident phosphorylation site localization using phosphoRS. J Proteome Res *10*, 5354-5362.